The Linnean Society of London
ZOOLOGICAL Journal of the Linnean Society

Integrative taxonomy resolves three new cryptic species of small southern African horseshoe bats (Rhinolophus)

Journal:	*Zoological Journal of the Linnean Society*
Manuscript ID	ZOJ-12-2017-3175.R1
Manuscript Type:	Original Article
Keywords:	craniometrics < Anatomy, genitalia < Anatomy, speciation < Evolution, mitochondrial DNA < Genetics, Natural hybridization < Genetics, Africa < Geography, cryptic species < Taxonomy
Abstract:	Examination of historical and recent collections of small Rhinolophus bats revealed cryptic taxonomic diversity within southern African populations previously referred to as R. swinnyi Gough, 1908 and R. landeri Martin, 1832. Specimens from Mozambique morphologically referable to R. swinnyi were phylogenetically unrelated to topotypic R. swinnyi from the Eastern Cape Province of South Africa based on cytochrome-b sequences and showed distinctive echolocation, baculum and noseleaf characters. Due to their genetic similarity to a previously reported molecular OTU from north-eastern South Africa, Zimbabwe and Zambia, we recognise the available synonym (R. rhodesiae Roberts, 1946) to denote this distinct evolutionary species. This new taxon is genetically identical to R. simulator K. Andersen, 1904 based on mtDNA and nuclear DNA sequences but can easily be distinguished on morphological and acoustic grounds. We attribute this genetic similarity to historical introgression, a frequently documented phenomenon in bats. An additional genetically distinct and diminutive taxon in the swinnyi s.l. group (named herein, R. gorongosae sp. nov.) is described from Gorongosa National Park, central Mozambique. Specimens from Mozambique referable based on morphology to R. landeri were distinct from topotypic landeri from West Africa based on mtDNA sequences, and acoustic, noseleaf and baculum characters. This Mozambique population is assigned to the available synonym R. lobatus Peters, 1952.

INTRODUCTION

Recent decades have seen an increase in the number of new species descriptions of mammals including bats in the region comprising Africa and the Western Indian Ocean Islands. In the 20 years preceding 2008, 22 new species of Afro-Malagasy bats were described (Hoffmann et al., 2009). This pace of discovery has intensified, with a further 35 new Afro-Malagasy species described between 2009 and 2017, 20 of them from the African mainland (African Chiroptera Report, 2015; references listed below). These recent discoveries span several families, including Hipposideridae (Goodman *et al.*, 2016), Miniopteridae (e.g., Goodman *et al*., 2008, 2011; Monadjem *et al*., 2013b), Molossidae (e.g., Goodman *et al*., 2010 ; Ralph *et al*., 2015), Pteropodidae (Nesi *et al*., 2013; Hassanin *et al*., 2015), Rhinolophidae (Benda & Vallo, 2012; Taylor *et al*., 2012; Kerbis Peterhans *et al*., 2013), and Vespertilionidae (e.g., Monadjem *et al*., 2013c; Brooks & Bickham, 2014; Decher *et al*., 2015; Goodman *et al*., 2017; Hassanin et al., 2017).

One reason for this burst of discoveries has been the use of multiple lines of evidence in resolving the species diversity of regional bat faunas, referred to as the integrative approach (Schlick-Steiner *et al*., 2010). Traditional morphological evidence alone, even established skull and dental characters, is in many cases unable to discriminate between cryptic species, although baculum (*os penis*) characters do distinguish many cryptic species of horseshoe bats (Cotterill, 2002; Taylor *et al*., 2012; Monadjem *et al*., 2013b). However, the inclusion of molecular data has radically altered the ability to distinguish morphologically similar species. With reference to bats, the use of morphological (including baculum), genetic and acoustic features together provides the integrative approach to advance taxonomy.

Molecular evidence contributes increasingly to resolve challenging taxonomic problems in bats, and particularly African horseshoe bats. Recent molecular studies have uncovered several new cryptic species and undescribed lineages of African horseshoe bats of the genus *Rhinolophus* Lacépède, 1799 (Stoffberg, Schoeman & Matthee, 2012; Taylor *et al*., 2012; Jacobs *et al*., 2013; Dool *et al*., 2016). Nevertheless, at least four species of *Rhinolophus* have been described based only on morphological differences (Kock, Csorba & Howell, 2000; Cotterill, 2002; Fahr *et al*., 2002; Kerbis Peterhans *et al*., 2013). In combination with sonar, cranial, dental and bacula characters, Taylor *et al*. (2012) employed molecular techniques to diagnose five genetically distinct lineages comprising the *R. hildebrandtii* complex, and so characterize four distinct new species in addition to *R. hildebrandtii sensu stricto*.

Echolocation calls of *Rhinolophus* spp. have a constant frequency (CF) component (Monadjem *et al.*, 2010), which has also been used to distinguish different taxa. For example, the morphologically similar *R. simulator* and *R. swinnyi* have distinctly dissimilar peak frequencies (Monadjem *et al.*, 2010), but differences in echolocation frequency are not infallible diagnostic characters. For example, variation in constant frequency within

species and species-complexes in this genus has been attributed *inter alia* to speciation (Taylor *et al.*, 2012; Jacobs *et al*., 2013), genetic drift (Odendaal & Jacobs, 2011), allometric effects (Stoffberg, Jacobs & Matthee, 2011) and environmental variables such as relative humidity (Mutumi, Jacobs & Winker, 2016).

Using several mitochondrial and nuclear DNA markers, Dool *et al*. (2016) showed that both *R. swinnyi* Gough, 1908 and *R. landeri* Martin, 1838 were paraphyletic. Topotypic *R. swinnyi* from the Eastern Cape Province of South Africa (type locality: Pirie Forest), was affiliated with the *R. capensis* group, while two specimens of *R.* cf*. swinnyi* (which they called cf*. simulator*) from Zambia and northern South Africa were affiliated more closely with nominate *R. simulator*. In the case of *R. landeri*, two specimens from Zimbabwe formed a sister lineage with *R. alcyone*, whilst two West African specimens of *R. landeri* (type locality: Equatorial Guinea) from Mali formed a distinct clade, which was sister to the *alcyone* and *landeri* complexes.

Informed by newly collected series of *R.* cf*. swinnyi* and *R.* cf*. landeri* from Mozambique and South Africa, the aim of this study was to review the status of above mentioned cryptic species, augmented by broader sampling, with the combined evidence of craniometric, morphological, acoustic, bacular, dental and molecular data. Here we diagnose the different taxa comprising the *landeri*, *simulator* and *swinnyi* species complexes, and we resurrect two distinct species from synonymy, and name a third new species using the integrative taxonomic approach. Of the two species-groups, *R. landeri* s.l. has a wide but sparse distribution encompassing much of western, eastern and south-central Africa. On the other hand, *R. swinnyi* s.l. is more restricted in range occurring in the eastern parts of the subcontinent from the southern reaches of the Democratic Republic of Congo to as far south as the Eastern Cape Province of South Africa (Monadjem *et al.,* 2010; African Chiroptera Report, 2015). Given the close genetic relationship between the new *R.* cf*. swinnyi* taxon and *R. simulator*, and as the two species are easily confused in the field, we included *R. simulator* s.l. K. Andersen, 1904, in this study, as well as topotypic samples of *R. swinnyi* and *R. landeri*.

MATERIALS AND METHODS

MOLECULAR ANALYSIS

PCR amplification and sequencing. DNA was extracted from each sample using a Zymogen DNA extraction kit (www.zymoresearch.com) according to the manufacturer's instructions. Specimen DNA was amplified via Polymerase Chain Reaction (PCR) using primers designed to amplify the cytochrome oxidase B gene. Mammalian cytochrome *b* (cyt *b*) primers were used, C3FF5 (5'ACCAATGMMATGAAAAATCATCGTT'3) and C3FF6 (5' TCTYCATTTYWGGTTTACAAGAC'3), to amplify and sequence cyt *b* regions and was derived from Irwin, Kocher & Wilson (1991). The PCR reactions for both markers contained 9.5 µl H_2O, 12.5 µl 2x EconoTaq buffer, 1 µl

forward and reverse cyt *b* primer (10 µM). The PCR thermal cycle was [95°C for 5 min], 30 x [(94°C for 30 s), (58°C for 45 s), (72°C for 45 s)] and [72°C for 10 min], [15°C for ∞]. PCR products for each sample were checked for quality and quantity using a Nanodrop 3000 spectrophotometer and subsequently run on a 1% agarose gel, using 1 µl of loading dye and 5 µl of PCR product per sample. Samples were then Sanger sequenced using an ABI 3730 capillary sequencer at Inqaba Biotechnical Industries (Pretoria, South Africa).

Sequence alignment and editing. Between 700 and 900 base pairs (bp) of the cyt *b* locus of the mtDNA cytochrome oxidase gene were amplified and sequenced for the *Rhinolophus* spp. samples. BioEdit version 7.0.9 (Hall, 1999) was used to align and edit the sequence electropherograms. The sequences were aligned using ClustalW (Larkin *et al*. 2007), and the resultant alignment checked and realigned by eye. Any remaining ambiguities were compared to their respective complement sequences, and corrected using the toggle translate function. The final alignments were trimmed to a length of 500 bp for the cyt *b* marker. New sequences are assigned Genbank Accessions

Phylogenetic and haplotype analysis. jModeltest (Guindon & Gascuel, 2003; Darriba *et al*., 2012) was used to search for the best fit model of evolution that fitted the genetic marker dataset. The GTR model of Tavare (1986) was chosen to construct the likelihood (ML) trees in MEGA v.7 (Kumar, Stecher & Tamura, 2016). MrBayes 3.1.2 (Ronquist & Huelsenbeck, 2003) was used to estimate a phylogenetic tree and to estimate the posterior probability of nodes using the same model of evolution with appropriate priors. The cyt *b* Bayesian trees were rooted using outgroups from other *Rhinolophus* spp. and additional sequences from relevant reference collections accessioned on GenBank were used as supplementary data (supplementary data S1). After re-alignment, including GenBank accessioned sequences, likelihood and parsimony analyses were performed. The likelihood and parsimony trees bootstrapped for 100 iterations, and genetic distances (corrected and uncorrected 'p') calculated using pair-wise comparisons of taxa, were completed in MEGA v.7 (Kumar *et al*., 2016). The Bayesian trees estimated with specimen sequences were created using four Markov chains of 1 000 000 generations each, sampled every 10 generations. After diagnostics indicated that all independent runs had converged, a consensus tree was constructed. The first 10 000 trees were discarded as burn in, and the rest of the genealogies used to construct a 50% majority-rule consensus tree. Minimum-spanning was used to construct a haplotype network using the cyt *b* sequence data with gaps coded as missing and with each node supplied with the number of specimens assigned to haplotypes per region by Popart (http://popart.otago.ac.nz).

MORPHOLOGICAL ANALYSIS

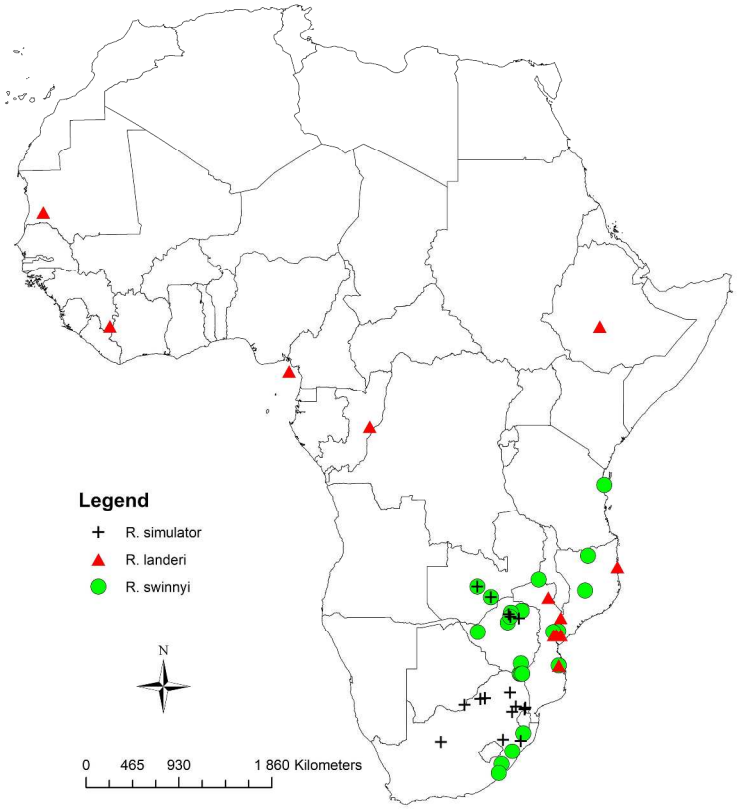

Figure 1. Map showing localities of R. swinnyi s.l. (triangles), R. landeri s.l. (circles) and R. simulator (crosses) sampled by this study. The locations of type specimens included in the study are denoted with arrows. See Supplementary Table S1 for list of localities, specimens and Genbank sequences included in the study

296x419mm (300 x 300 DPI)

Specimens. We examined recent collections of skins and skulls of three small rhinolophid species (*Rhinolophus swinnyi* s.l., *R. simulator* s.l. and *R. landeri* s.l.) from across the continental range of these species, with special emphasis on southern African subregion (Fig. 1). The associated voucher specimens are held in the Durban Natural Science Museum, Durban (DM), Field Museum of Natural History , Chicago (FMNH) and Ditsong National Museum of Natural History, Pretoria (formerly Transvaal Museum; TMSA) (Table S1). We also included measurements from relevant type specimens and other representative series in the collections of The Natural History Museum, London (formerly British Museum [Natural History]; (BMNH), the Muséum National d'Histoire Naturelle, Paris (MNHN), the Zoologisches Museum, Berlin (ZMB), the Natural History Museum of Zimbabwe, Bulawayo (NMZB) and the Ditsong National Museum of Natural History (Table S1). We only selected adults for further measurement and analysis, which we defined based on the degree of tooth wear and extent of ossification of finger bone epiphyses (Taylor *et al*., 2012).

Morphometric analyses. We used two morphometric approaches: analysis of traditional linear cranial measurements, as well as landmarks placed on lateral images of specimen crania. We analysed variation in a sample of 124 intact skulls using 10 craniometric variables (see definitions below) and standard external measurements obtained from field notes of AM, JAG, LRR, MCS, PJT and SMG, although a few measurements were obtained from museum specimen labels. Because the premaxilla was often absent in museum skulls, numerous specimens could not be measured for two standard skull variables: greatest length of skull measured dorsally from occiput to anterior point of skull (GSL) and condyloincisive length from occipital condyles to front of incisors (CIL). For this reason, herein, we did not include these two variables in statistical analyses, but certain comparisons were made using these two measurements. The following 10 cranial measurements were taken to the nearest 0.01 mm using either Mitutoyo or Tesa digital callipers with accuracy of 0.01 mm: 1) condylocanine length from occipital condyles to front of canines (CCL); 2) zygomatic width, the greatest distance across the zygoma (ZW); 3) mastoid width, the greatest distance across the lateral projections of the mastoid processes (MW); 4) width of maxilla between outer edges of M3 (M3M3); 5) braincase width measured at dorsal surface of posterior root of zygomatic arches (BCW); 6) least interorbital width (IOW); 7) upper toothrow length from anterior surface of C to posterior surface of M3 (C1M3); 8) greatest width across anterior lateral nasal inflations (NW); 9) length from occipital condyles to front of nasal inflations (NL); and 10) height of nasal inflation directly above the anterior cingulum of M2 (NH). To include data from type specimens and others for which only five cranial measures (CCL, ZW, MW, M3M3, C1M3) were available, principal component analysis (PCA) was repeated for these five variables resulting in a final sample of 160 skulls (Table S1).

Because both multivariate and univariate analyses failed to detect significant sexual dimorphism in either cranial or external measurements of the three taxa; adult males and females were pooled. To visualise intraspecific and interspecific variation in multidimensional space of linear measurements, principal component analysis (PCA) was carried out on log-transformed cranial variables using the programme PAST (Hammer, Harper & Ryan, 2001).

Geometric morphometric analysis. We used this approach to explore intra- and inter-specific differences in cranial size and shape from digital images of the left lateral profile of 118 *Rhinolophus* spp. skulls (Supplementary information: Table S1). Digital images were captured using a Canon Powershot A650 IS digital camera mounted on a tripod (x6 optical zoom, 5 megapixel resolution, 25 mm focal length, macro function). Eighteen homologous landmarks were captured in two dimensions (2D) from cranial images using tpsDig, v.2.17 (Rohlf, 2013). Landmarks were described as follows: 1) junction of maxillae and anterior margin of C1; 2) junction of maxillae and anterior margin of PM2; 3) posterior margin of maxillae/end of toothrow; 4) junction of maxillae and jugal process; 5) junction of squamosal and auditory meatus; 6) highest point of external bullae; 7) junction of bullae and occipital condyle; 8) longest point of condyle; 9) anterior margin of foramen magnum; 10) posterior margin of foramen magnum; 11) junction of sagittal and lambdoidal crests; 12) sharpest point of parietals; 13) junction of parietal and temporal; 14) highest point of braincase/temporal region; 15) most posterior point of the interorbital constriction; 16) base of nasal inflation; 17) highest point of nasal inflation; and 18) junction of maxillae and nasal inflation. A Generalized Procrustes Analysis (GPA) of the landmark data set and principal component analysis (PCA) of the total shape matrix was conducted using MorphoJ software (Klingenberg, 2011). Taxon-specific thin plate splines illustrating global and localised cranial shape characteristics, exaggerated 3x, were generated using tpsREGR, v.1.38 (Rohlf, 2011).

Morphological comparisons. In additional to morphometric analysis of continuous characters, we scored the following qualitative characters: the position (external or within toothrow) and relative size of the small anterior upper premolar, and the presence or absence of apical tufts (distinct cluster of stiff orange hairs located in the armpit of certain male *R. landeri* individuals). We provided detailed descriptions of the noseleaf morphology of taxa delineated by genetic and morphometric analyses. The terminology of the connecting process structure and protuberance and the shape of the lancet are based on Csorba, Ujhelyip & Thomas (2003) and Happold & Cotterill (2013).

Baculum morphology. Thirty-three bacula were prepared from alcohol-preserved adult male specimens following the methods of Hill & Harrison (1987) and Kearney *et al.* (2002), with slight modification of the procedures to clear penile tissue (specimens listed in Table S1). The glans penis was removed and hydrated in distilled water for 24 hrs. The penile tissue was then macerated for 36-48 hrs in a 5% KOH solution with Alizarin red stain. The stained baculum was cleared of the macerated tissue by hand using fine forceps. Each baculum was placed on a stage micrometer and was photographed in the dorsal, lateral and ventral views using a dissecting microscope and an ocular mounted MU500 5 M pixel digital USB microscope camera (AmScope, USA). Eight measurements were recorded from digital images using the "Length Measurement" feature of the ToupView software program (ToupTek Phototonics): 1) total length; 2) greatest base width (dorsal view); 3) greatest base width (lateral view); 4) widest region along the shaft; 5) narrowest region along the shaft; 6) widest region of shaft tip; 7) greatest length of the dorsal basal notch; and 8) base height. In specimens without a distinct and/or expanded shaft tip, the tip was regarded as occupying the uppermost portion of the shaft (approximately 20% of the entire shaft). Measurements were log-transformed and subjected to PCA using IBM SPSS Statistics v. 21.0 (IBM Corp). As sample size was in several cases low, a Kaiser-Meyer-Olkin (KMO) test was performed to determine sampling adequacy for each variable and the overall model (Kaiser, 1974). Line drawings of selected bacula were made from digital images of the respective views that were representative of the different taxa.

ACOUSTIC ANALYSIS

Acoustic recordings of most bats were obtained using one of the following three time expansion bat detectors: Pettersson D1000X, Pettersson D980 ultrasound recorders (Pettersson Electronik AB, Uppsala, Sweden) or Avisoft Ultrasound 116Hb bat detector (Avisoft Bioacoustics, Berlin, Germany). Sampling rate was set to 300 kHz, with 16-bit Analog-to-Digital converter. Recorded calls were analysed with BatSound Pro software (Pettersson Electronik AB, Uppsala, Sweden). The dominant harmonic from each call was taken from the fast Fourier transform power spectrum. A Hanning window was used to eliminate effects of background noise. Peak echolocation frequency was measured from the maximum amplitude of the power spectrum. Bats were recorded hand-held. The echolocation calls of the two specimens of *R. landeri* from Liberia were recorded using an Anabat SD2 detector (Titley Electronics, Ballina, Australia), whilst the bats were held, separately, in a small cloth bag. Calls were analysed using ANALOOK software (Chris Corben, ver. 4.8, http://www.hoarybat.com). The frequency of the constant frequency (CF) component [= maximum frequency F(max)] was measured.

RESULTS

MOLECULAR ANALYSIS

Based on cytochrome *b* (cyt *b*) sequences (Figs 2, 3), *Rhinolophus* cf. *swinnyi* collected in Mozambique (Malashane Cave, Chihalatan Cave and Gorongosa National Park) were phylogenetically distinct from topotypical *R*. *swinnyi* from the Eastern Cape Province, South Africa; the latter has *R*. *capensis* as its sister species. Specimens assigned to cf. *swinnyi* from Malashane Cave and Chihalatan Cave are genetically very close to Genbank sequences of cf. *swinnyi* obtained from Zimbabwe, Zambia and the Pafuri region of the extreme north of South Africa (see Dool *et al*., 2016), allowing us to assign this lineage to the taxon *R*. *rhodesiae* Roberts, 1946 described from Bezwe River in southern Zimbabwe, and previously classified as *R. s, rhodesiae* (Ellerman, Morrison-Scott & Hayman 1953). However, two cf. *swinnyi* from Gorongosa National Park form a highly distinctive group separated by uncorrected p-distances of 13.2% and 7.2% from topotypic *R*. *swinnyi* and *R*. *rhodesiae*, respectively (Table 1). Despite these two individuals being relatively genetically distinct (p = 1.8%) from each other (Figs. 2, 3), we refer to them both as the new species (described below), *Rhinolophus gorongosae* sp. nov. The species is closely affiliated with topotypic *R*. *landeri* from Liberia, West Africa, but still genetically distant (15.0%; Table 1).

Rhinolophus cf. *landeri* from Malashane Cave, Chihalatan Cave and Gorongosa National Park form a homogeneous group that is phylogenetically distinct from West African *R*. *landeri* (Mount Nimba, Liberia). These three localities in central and eastern Mozambique fall in close geographic proximity to the type locality of *R*. *lobatus* at Sena, Mozambique, on the south bank of the Zambezi River (Peters, 1852) (Figs. 1,2; Table S1). We therefore refer to this taxon to *R*. *lobatus*.

Enigmatically, individuals of *R. rhodesiae* are genetically inseparable (Fig. 2, Table 1: p = 0.6%) from the morphologically distinct species, *R. simulator*, a result also obtained by Dool *et al*. (2016) informed by mitochondrial and nuclear evidence.

MORPHOMETRIC VARIATION

External morphology. External characters (Table 2) confirm *Rhinolophus swinnyi* s.l. (including *R. swinnyi* s.s., *R. gorongosae* sp. nov. and *R. rhodesiae*) to be smaller (total length always < 80 mm; 61–79 mm) than *R*. *simulator* (total length 77–79 mm) and *R*. *landeri* s.l. (total length typically > 80 mm; 79–87 mm), as also reflected in the PCA of cranial variables (Fig. 4, see below). Within *R*. *swinnyi* s.l., as also clearly reflected in the cranial data (see below), the genetically-distinct Gorongosa National Park population (*R. gorongosae* sp.nov.) is distinctly smaller in external measurements (e.g. mean total length 68 mm) than both *rhodesiae* from Malashane and Chihalatan Caves (mean total length 75 mm) and *swinnyi* s.s. from South Africa (mean total length 73 mm). Specimens of *R*. *lobatus* from Gorongosa National Park appear smaller externally (total length 72–82 mm, mean 76 mm) than *R*. *lobatus* from Malashane and Chihalatan Caves (total length 79–87 mm, mean 82 mm; Table 2) with some overlap.

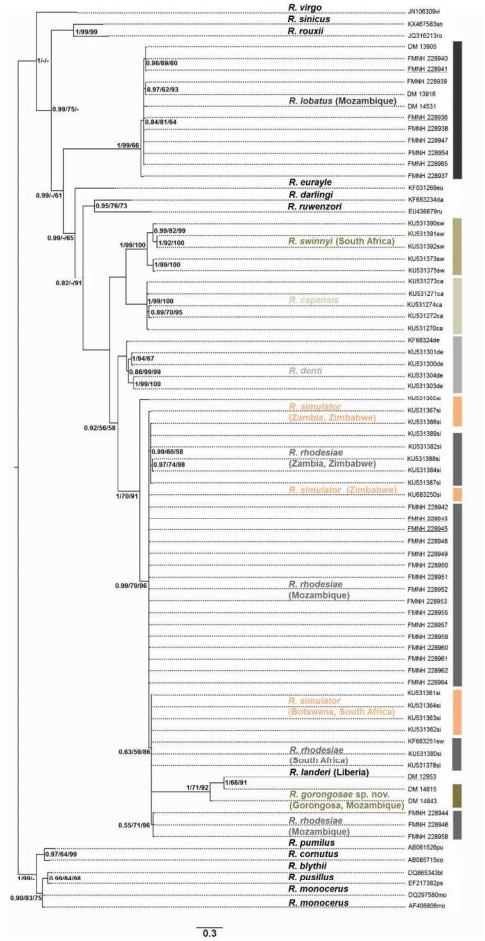

Figure 2. Bayesian tree of partial Cytochrome b sequences, with nodal support values based on Bayesian probabilities and bootstrap values for Maximum Likelihood and Maximum Parsimony. Samples included in all analyses (molecular, morphometric and bacular) are underlined.

297x420mm (300 x 300 DPI)

Table 1. Mean uncorrected p-distances (below) diagonal and Kimura 2-parameter model-corrected distances (above diagonal) based on 667 cytochrome b (cyt *b*) sequences between eight recognised and newly proposed species of small African *Rhinolophus* bats. Within-species uncorrected p-distances provided in parentheses on the diagonals, except for *R. landeri* where only one individual was available.

	simulator	*denti*	*rhodesiae*	*swinnyi*	*capensis*	*landeri*	*lobatus*	*gorongosae* sp. nov.
simulator	(0.009)	0.043	0.006	0.093	0.087	0.256	0.156	0.077
denti	0.041	(0.021)	0.043	0.077	0.070	0.243	0.141	0.102
rhodesiae	0.006	0.041	(0.002)	0.094	0.087	0.256	0.156	0.076
swinnyi	0.086	0.071	0.086	(0.011)	0.060	0.244	0.143	0.147
capensis	0.080	0.066	0.080	0.057	(0.006)	0.241	0.147	0.135
landeri	0.215	0.206	0.215	0.207	0.205	NA	0.237	0.168
lobatus	0.138	0.126	0.137	0.128	0.131	0.202	(0.003)	0.194
gorongosae sp. nov	0.073	0.095	0.072	0.132	0.122	0.150	0.168	(0.018)

Table 2. Summary statistics for six external and three cranial variables (in mm), mass (in g) and echolocation peak frequency for museum type specimens and series of taxa sampled in this study in the *swinnyi*, *simulator* and *landeri* groups. Except in the case of type specimens and certain series where indicated, all measurements were taken by the authors of this paper. * Data obtained from Taylor (2005). See Materials & Methods for definitions of museum acronyms.

Taxon group or type	Total length (mm)	Tail length (mm)	Ear length (mm)	Hindfoot length (mm)	Forearm length (mm)	Noseleaf width (mm)	Peak frequency (kHz)	Mass (g)	Greatest skull length (mm)	Condylo-canine length (mm)	Zygomatic width (mm)
R. gorongosae sp. nov. (holotype: DM 14820)	66.5	26	18	7.5	41.5	7	-	5.1	-	15.2	8.25
R. gorongosae sp. nov.	**67.6** ± 3.8, n=15, 61–78	24.7 ± 1.6, n=15, 22–27	17.3 ± 2.2, n=15, 12.5–22	8.1± 0.5, n=15, 7.5–9.0	41.3 ± 1.6, n=15, 38.5–44.5	7.1 ± 0.3, n=15, 7–8	106.2 ± 1.5, n=16, 103.5-107.8	5.6 ± 0.5, n=15, 4.5–6.6	-	15.1± 0.19,n=7, 14.8–15.2	8.39 ± 0.16, n=8, 8.13–8.56
R. swinnyi Gough 1908 (co-types: TMSA 1021, 1022)	60–61	18–19	18	8	40.8–41.8 (40–40.7 in description)	-	-	-	17.5	15.5	8.73–8.97, n=2
R. swinnyi (South Africa)	73.0 ± 1.7, n=3, 71–74	22.0 ± 3.8, n=6, 18.3–27	18.8 ± 1.6, n=6, 17.2–21.6	8.5 ± 0.3, n=6, 8.2–9.1	43.6 ± 1.1, n=9, 41.7–45.0	-	105.9 ± 0.7, n=6, 104.9-106.7	-	17.7 ± 0.5, n=10, 16.8–18.0	15.4 ± 0.45,n=10, 14.3–16.0	9.1 ± 0.2, n=11, 8.7–9.2
R. s. rhodesiae Roberts 1946 (holotype: TMSA 1325)	74	22	15	-	41.4 (40.5 in description)	-	-	-	17.6	14.9	8.34
R rhodesiae (Chihalatan/Malashane)	74.8 ± 5.4, n=20, 68–79	24.4 ± 1.5, n=20, 23–29	19.9 ± 0.6, n=20, 19–21	6 ± 0, n=20, 6	44.2 ± 0.9, n=20, 43–45	7.2 ± 0.7, n=18, 6.2–8.1	100.1±1.0, n-8, 99.1-102	5.7 ± 0.33, n=20, 4.9–6.1	17.8 ± 0.4, n=13, 17.2–18.6	15.4± 0.22,n=13, 15.1–15.7	8.7 ± 0.1, n=20, 8.46–8.96
R. landeri Martin 1838 (holotype: BMNH 1847.5.7.49)	-	-	-	-	-	-	-	-	16.7 (broken)	-	-
R. landeri (Liberia)	79–81, n=2	27, n=1	18–19, n=2	-	42–43.9, n=2	-	104.3 ± 0.4, n=2, 104-104.6	7.8–8.5, n=2	18.8–18.9, n=2	16.3–16.6, n=2	9.44–9.62, n=2
R. l. lobatus Peters 1852 (syntypes: ZMB 24922, 24927	81.7 ± 2.9, n=3, 80–85	25.0 ± 1.0, n=3, 24–26	16.0 ± 0, n=3, 16	9.8 ± 0.29, n=3, 9.5–10	45.2 ± 0.76, n=3, 44.5–45	7.1 ± 0.14, n=3, 7–7.25	-	-	-	-	-
R. lobatus (Chihalatan/Malashane)	82.5 ± 2.45, n=9, 79–87	26.4 ± 2.30, n=9, 23–31	19 ± 1.12, n=9, 17–20	6.89 ± 0.79, n=9, 6–8	47 ± 1.22, n=9, 46–49	7.5 ± 0.56, n=9, 6.6–8.3	106.8± 0.4, n=4, 106.5-107	7.5, n=9, 7–9	19.0 ± 0.41, n=9, 18.5–19.5	16.4± 0.16, n=9, 16.2–16.5	9.5 ± 0.23, n=9, 9.3–9.9
R. lobatus (Gorongosa)	75.8 ± 2.6, n=26, 71.5–81.5	25.2 ± 3.3, n=26, 21.4–28.0	17.3 ± 1.3, n=26, 13.7–19.5	9.7 ± 0.9, n=26, 7.9–11.7	45.2 ± 1.5, n=26, 43.0–49.5	7.6 ± 0.4, n=26, 7.1–8.1	105.1 ± 1.8, n=20, 101.9-107.6	8.2 ± 1, n=26, 5.2–9.5	18.9 ± 0.33, n=12, 18.4–19.5	16.5± 0.29, n=12, 16.0–17.0	9.8 ± 0.21, n=12, 9.4–10.1
R. simulator (holotype: BMNH 2.2.7.10)	-	25.7	20	-	41.5 (43.5 in description)	8.3	-	-	18.9	16.2	8.8
R. simulator (South Africa)	78 ± 0.6, n=6, 77–79	24.8 ±2.0, n=6, 22–28	19.5 ±1.3, n=6, 17.2–21.1	10.0 ± 0.5, n=5, 9.4–10.4	44.0± 1.0, n=6, 42.7–45.8	-	83.4 ± 0.6, n=6, 82.6-83.8		18.9 ± 0.48, n=11, 18.3–19.7	16.6 ± 0.32,n=13, 16.1–17.2	9.0± 0.2, n=13, 8.8–9.4

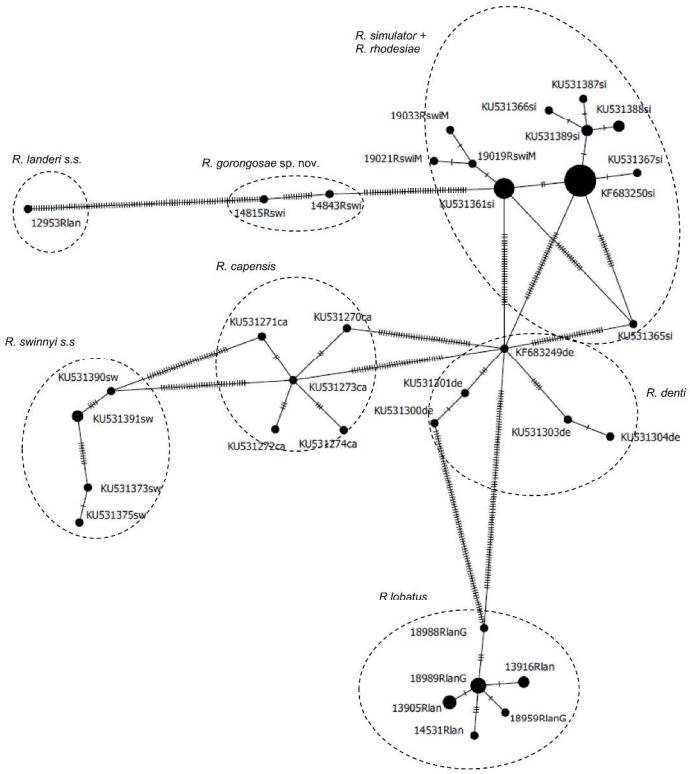

Fig. 3 Haplotype network using minimum-spanning inference method based on 667 base pairs of cyt-b.

297x420mm (300 x 300 DPI)

While the same trend is present in tail and ear lengths, the opposite is true for hind foot length, which is larger in the Gorongosa National Park population than in those from Malashane and Chihalatan Caves (Table 2).

Intraspecific craniometric variation. A PCA of 10 log-transformed craniodental variables revealed considerable overlap in size between males and females in both *R. swinnyi* s.l. and *R. landeri* s.l. (Supplementary information: Fig. S1). Furthermore, means of 10 craniodental variables showed no significant sexual dimorphism in any external or cranial variables for either species (data from *t*-tests, not shown). For example, forearm length was 44.0 mm (42.8–45.0 mm, n = 15) and 43.7 mm (42.0–45.0 mm, n = 10) in female and male *R. rhodesiae* from Mozambique (Malashane and Chihalatan Caves and Mount Inago), respectively (t_{23} = 0.65, p > 0.05). In *R. lobatus* from Mozambique (Malashane and Chihalatan Caves and Muchena), forearm length was 46.6 mm (44.4–49.0 mmm, n = 9) and 45.5 mm (43.4–46.0 mm, n = 5) in females and males, respectively (t_{12} = 1.30, p > 0.05). These values fall within the range reported by Monadjem *et al*. (2010) for *R. swinnyi* s.l. but above the mean (44.0 mm) and range of 42.0–47.8 mm for *R. landeri* s.l. (Monadjem *et al*., 2010). In terms of cranial size, mean CCL of *R. rhodesiae* females was 15.4 mm (15.0–15.7 mm, n = 15) and for males 15.4 mm (15.1–15.7 mm, n = 12) (t_{23} = 0.77, p > 0.05), and in *R. landeri*, for females 16.4 mm (15.9–16.8 mm, n = 9) and for males 16.3 mm (16.2–16.5 mm, n = 5) (t_{12} = -0.12, p > 0.05). These values are close to the published ranges and means of condylo-incisive length (CIL) in Monadjem *et al.* (2010) for both species. Based on our data, CCL is typically 0.1–0.7 mm larger than CIL in any one skull, suggesting that our samples referred to *R. swinnyi* s.l. and *R. landeri* s.l. might be slightly smaller than recorded by Monadjem *et al*. (2010).

Interspecific craniometric variation. A PCA based on 10 log-transformed cranial variables clearly resolved three groups commensurate with *R. swinnyi* s.l., *R. landeri* s.l. and *R. simulator* s.l. (data not shown but available from PJT on request). To include data from type specimens for which only five cranial measures were available, PCA was repeated with only these five variables, which resolved the same three distinct groups (Fig. 4). Specimens of *R. swinnyi* s.l. could be distinguished from *R. landeri* s.l. and *R. simulator* based on their smaller size (all variable loadings on the first component were positive and *R. swinnyi* s.l. plotted to the left; Fig. 4, Table 3). Condylocanine skull length (CCL) was always < 16.0 mm in *R. swinnyi* s.l. and > 16.0 mm in *R. simulator* and *R. landeri* s.l. (Table 2). There was noticeable variation within *R. swinnyi* s.l., which occupied a much broader morphometric space than the other two taxa (*R. simulator* s.l. and *R. landeri* s.l.). In particular specimens from Gorongosa National Park herein designated *R. gorongosae* sp. nov., were distinctly smaller-sized than other members of this group. Animals referable to *R. rhodesiae*, as identified by genetic analysis, overlapped considerably with *R. swinnyi* s.s. (Fig. 4). The holotype of *rhodesiae* (TMSA 1325) from Bezwe River in Zimbabwe plotted within the range of variation of

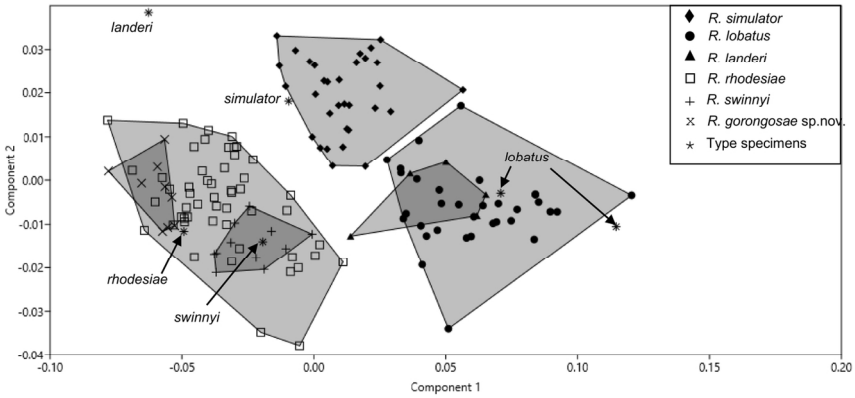

Figure 4. PCA variation for five log-transformed cranial variables for six proposed small southern Africa Rhinolophus spp. defined on molecular and morphological grounds.

140x95mm (300 x 300 DPI)

Table 3. Variable loading matrix for PCA of interspecific variation in three small African *Rhinolophus* spp. See Fig. 5 for details.

Variable	PC 1	PC 2	PC 3
Condylo-canine length (CCL)	0.337	0.509	0.254
Zygomatic width (ZW)	0.520	-0.392	0.353
Mastoid width (M)	0.380	0.061	0.562
Width of maxilla between outer edges of M3 (M3M3)	0.519	-0.490	-0.518
Upper toothrow length (C1M3)	0.450	0.586	-0.476

specimens referred genetically to *rhodesiae*, confirming the validity of the name. Specimens assigned to *R. landeri* s.s. from west, central, north and north-eastern Africa and *R. lobatus* from southern Africa overlapped considerably in size. As it is a sub-adult, the *landeri* holotype from Equatorial Guinea was distinctly smaller-sized than other *landeri* individuals, and is therefore not informative. The two co-types of *lobatus* from Sena River, Mozambique, plotted within the range of variation of specimens referred genetically to *lobatus*, confirming the validity of this name. Although *R. simulator* overlapped slightly in size with *R. landeri* s.l. (Fig. 4), specimens of *R. simulator* grouped separately from those of *R.* cf. *landeri* on PC2; more positive scores are associated with a disproportionately longer and narrower palate/toothrow (high positive loading for CM3 and high negative loading for M3M3) (Table 3b).

Geometric morphometric variation. A PCA of 2D cranial landmark data recovered six partially overlapping groups corresponding to *R. gorongosae* sp. nov., *R. landeri*, *R. lobatus*, *R. simulator*, *R. rhodesiae* and *R. swinnyi* (Fig. 5). The type specimens of *rhodesiae* and *swinnyi* fell within the range of variation of the corresponding taxa defined on genetic grounds (see below). Deformation grids provide graphical representation of shape changes associated with PC 1 (from left to right) and those along PC 2 (bottom to top) (Fig. 5), as well as an illustration of overall cranial morphology of the different taxa as identified by PCA (Fig. 6). The diminutive Gorongosa National Park animals had a reduced foramen magnum as indicated by landmarks (LMs) 8–10, a noticeable depression along the parietal region (LM 13), low set bullae (LMs 5–7), and a narrow and high set nasal inflation with a sharp slope from the nasal inflation to the maxillae (LMs 1–18). The braincase of *R. gorongosae* sp. nov., in relation to *R. rhodesiae* and *R. swinnyi*, was narrower (LMs 6 and 14). *Rhinolophus swinnyi* s.s. had a dorsally expanded braincase due to the elevated positions of LMs 12–14, a broad foramen magnum (LMs 9–10), high set bullae (LMs 5–7), and a short and steeply inclined frontal region (LMs 14–15). The nasal inflation was posteriorly set and small (LMs 15–17). There was a short slope from the nasal inflation to the maxillae (LMs 17–18), and anterior margin of the maxillae was recessed (LM 1). *Rhinolophus rhodesiae* presented with an expanded braincase (LMs 10–14), relatively high positioned LM 12, elongated frontal region (LMs 14–15), wide bullae (LMs 5–7), and a narrowed nasal inflation (LMs 16–18).

Rhinolophus landeri from West Africa was distinguished from *R. lobatus* from south-eastern Africa by a broader rostrum (LMs 1, 2, 4 and 18), wider and higher set tympanic bullae (LMs 5–7), noticeably shortened foramen magnum (LMs 9–10), and a more rounded posterior portion of the braincase (LMs 10–14). The taxon had a narrow nasal inflation (LMs 16–18), with a steeply inclined slope from the highest point of the nasal inflation to the maxillae (LMs 17–18). In relation to *R. landeri*, *R. lobatus* had a less rounded braincase with higher positioned lambdoidal crests (LMs 10–14), and less steeply inclined anterior margin of the nasal inflation (LMs 17–18).

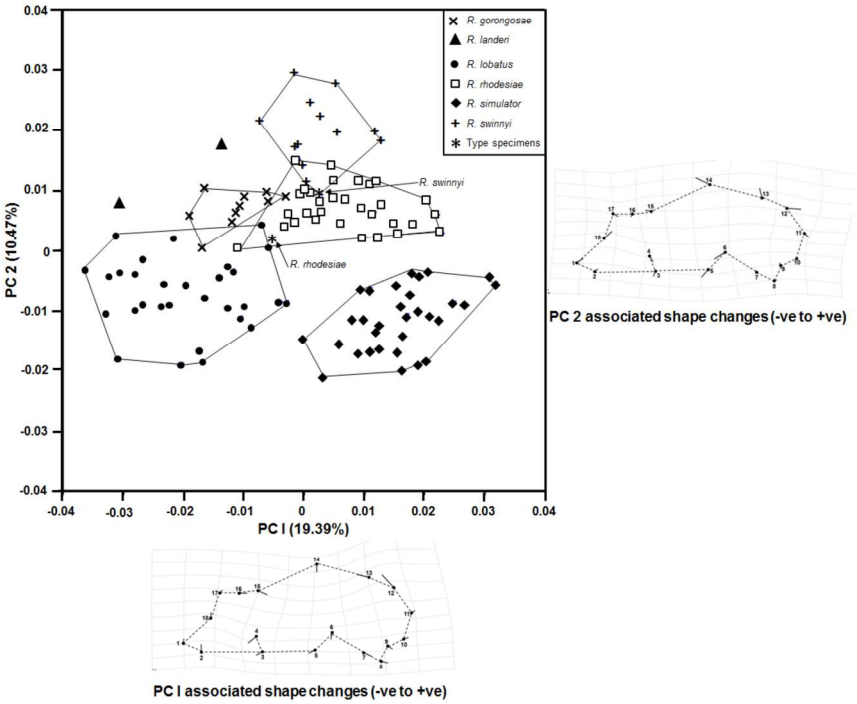

Figure 5. Biplot showing the first and second principal components from a PCA of 2D landmark data for small southern Africa Rhinolophus spp., including data from type specimens of R. swinnyi and R. s. rhodesiae. Deformation grids illustrate cranial shape changes associated with each PC.

177x152mm (300 x 300 DPI)

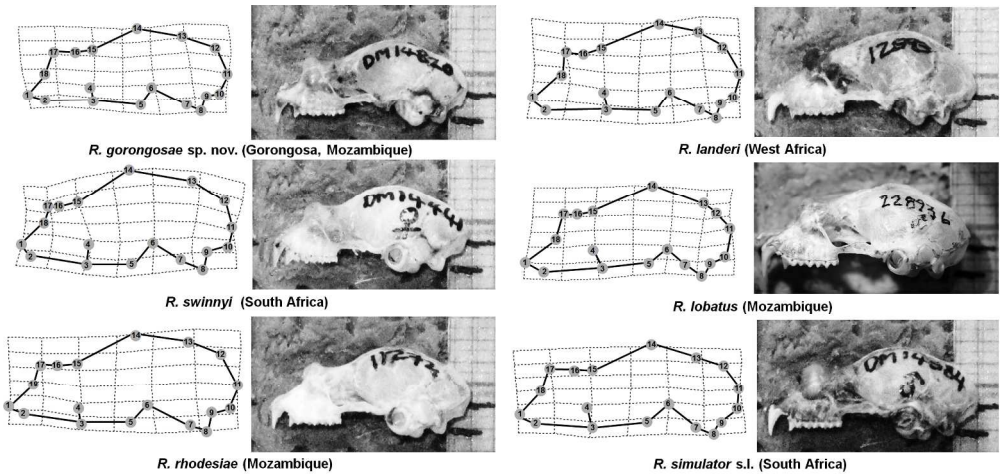

Figure 6. Overall lateral cranial morphology of small southern African Rhinolophus taxa as illustrated by deformation grids (exaggerated 3x).

649x309mm (96 x 96 DPI)

Table 4. Variable loading matrix for PCA of bacular morphological variation in three small African *Rhinolophus* spp.

Character	PC 1	PC 2	PC 3
Total length (dorsal)	0.867	0.349	0.183
Greatest base width (dorsal)	0.653	0.492	0.311
Greatest base width (lateral)	0.751	0.413	0.179
Greatest shaft width (dorsal)	0.188	0.194	0.934
Narrowest shaft width (dorsal)	0.351	0.878	0.167
Greatest tip width (dorsal)	0.444	0.660	0.423
Height of basal notch (dorsal)	0.471	0.281	0.223
Height of base (dorsal)	0.695	0.319	0.483

Table 5. Bacula measurements for 33 individuals of three small African *Rhinolophus* taxa. Mean, standard deviation, range and sample sizes are provided. All measurements recorded in mm. Numbers in superscript refer to the position of taxa in Fig. 7.

Taxon	Total length (dorsal)	Greatest base width (dorsal)	Greatest base width (lateral)	Greatest shaft width	Narrowest shaft width	Greatest tip width	Height of basal notch (dorsal)	Height of base
R. gorongosae sp. nov. (Gorongosa, Mozambique)	2.00 ± 0.11, n=3 1.91 – 2.12	0.53 ± 0.01, n=3 0.52 – 0.54	0.48 ± 0.04, n=3 0.43 – 0.50	0.22 ± 0.02, n=3 0.20 – 0.23	0.11 ± 0.01, n=3 0.10 – 0.12	0.22 ± 0.02, n=3 0.20 – 0.23	0.11 ± 0.02, n=3 0.09 – 0.12	0.41 ± 0.02, n=3 0.38 – 0.43
R. swinnyi (Eastern Cape / KwaZulu-Natal, South Africa)	2.06 ± 0.09, n=4 1.97 – 2.17	0.37 ± 0.06, n=4 0.45 – 0.60	0.37 ± 0.02, n=4 0.35 – 0.40	0.18 ± 0.02, n=4 0.16 – 0.21	0.12 ± 0.03, n=4 0.10 – 0.17	0.23 ± 0.05, n=4 0.17 – 0.29	0.07 ± 0.01, n=4 0.06 – 0.09	0.38 ± 0.08, n=4 0.32 – 0.49
R. rhodesiae (Chihalatan Cave, Mozambique / KwaZulu-Natal, South Africa)	2.59 ± 0.08, n=7 2.50 – 2.70	0.93 ± 0.06, n=7 0.83 – 0.99	0.83 ± 0.03, n=7 0.80 – 0.88	0.33 ± 0.03, n=7 0.28 – 0.37	0.19 ± 0.02, n=7 0.17 – 0.21	0.23 ± 0.02, n=7 0.19 – 0.26	0.20 ± 0.03, n=7 0.17 – 0.23	0.65 ± 0.05, n=7 0.59 – 0.74
R. landeri (Mount Nimba, Liberia)	2.29, n=1	0.88, n=1	0.78, n=1	0.27, n=1	0.18, n=1	0.30, n=1	0.15, n=1	0.72, n=1
R. lobatus[1] (Gorongosa / Chihalatan Cave, Mozambique)	2.57 ± 0.07, n=3 2.51 – 2.65	0.94 ± 0.04, n=3 0.91 – 0.99	0.97 ± 0.02, n=3 0.96 – 1.00	0.29 ± 0.02, n=3 0.28 – 0.32	0.22 ± 0.02, n=3 0.20 – 0.24	0.35 ± 0.02, n=3 0.32 – 0.37	0.17 ± 0.01, n=3 0.17 – 0.18	0.92 ± 0.01, n=3 0.92 – 0.92
R. cf. *lobatus*[2] (Gorongosa / Pemba, Mozambique)	2.96 ± 0.05, n=2 2.92 – 2.99	1.12 ± 0.00, n=2	1.22 ± 0.03, n=2 1.20 – 1.24	0.39 ± 0.01, n=2 0.38 – 0.39	0.22 ± 0.03, n=2 0.20 – 0.24	0.41 ± 0.01, n=2 0.41 – 0.42	0.27 ± 0.01, n=2 0.27 – 0.28	0.91 ± 0.01, n=2 0.90 – 0.92
R. cf. *lobatus*[3] (Gorongosa, Mozambique)	1.98 ± 0.00, n=2 1.98 – 1.98	0.42 ± 0.02, n=2 0.41 – 0.43	0.53 ± 0.01, n=2 0.52 – 0.53	0.28 ± 0.01, n=2 0.27 – 0.29	0.16 ± 0.00, n=2 0.16 – 0.16	0.30 ± 0.01, n=2 0.29 – 0.31	0.15 ± 0.00, n=2 0.15 – 0.15	0.48 ± 0.02, n=2 0.47 – 0.50
R. cf. *lobatus*[4] (Gorongosa / Malashane Cave, Mozambique)	1.98 ± 0.26, n=2 1.80 – 2.16	0.50 ± 0.03, n=2 0.48 – 0.52	0.52 ± 0.09, n=2 0.46 – 0.58	0.22 ± 0.03, n=2 0.20 – 0.24	0.13 ± 0.01, n=2 0.13 – 0.14	0.22 ± 0.04, n=2 0.19 – 0.24	0.14 ± 0.03, n=2 0.12 – 0.16	0.43 ± 0.05, n=2 0.40 – 0.47
R. simulator[5] (South Africa/Zimbabwe)	2.48 ± 0.18, n=6 2.20 – 2.69	0.82 ± 0.11, n=6 0.61 – 0.94	0.77 ± 0.05, n=6 0.67 – 0.82	0.24 ± 0.03, n=6 0.21 – 0.30	0.18 ± 0.02, n=6 0.14 – 0.20	0.29 ± 0.03, n=6 0.24 – 0.33	0.24 ± 0.05, n=6 0.16 – 0.29	0.68 ± 0.13, n=6 0.50 – 0.90
R. simulator[6] (KwaZulu-Natal, South Africa)	2.61 ± 0.15, n=3 2.43 – 2.70	0.98 ± 0.02, n=3 0.96 – 1.00	0.83 ± 0.05, n=3 0.78 – 0.88	0.24 ± 0.01, n=3 0.24 – 0.25	0.16 ± 0.00, n=3 0.15 – 0.16	0.29 ± 0.03, n=3 0.25 – 0.32	0.29 ± 0.01, n=3 0.28 – 0.31	0.90 ± 0.09, n=3 0.80 – 1.00

Rhinolophus simulator s.l. was characterised by an elongated cranium, with a distinctly widened nasal inflation (LMs 16–18), and broad tympanic bullae (LMs 5–7).

Bacular morphology. The KMO statistic = 0.88, indicating that the factors extracted by PCA accounted for the majority of sample variance. PCA of the eight bacular measurements delimited ten groupings varying in bacular length (PC1) and width (PC2), and which corresponded with all the taxa recognised in this study (Tables 4 and 5, Figs 7 and 8). In addition, four highly distinct groupings (bacular types, numbered 1–4 in Table 5 and Fig. 7) were detected within specimens referred to *R. lobatus* from Mozambique, and two distinct bacular types (labelled 5–6 in Table 5 and Fig. 7) were detected within *R. simulator* from South Africa and Zimbabwe. Bacular morphometric groups identified in Fig. 7 correspond to clearly recognisable morpho-types as indicated by the drawings in Fig. 8. Within *swinnyi* s.l. (*swinnyi*, *rhodesiae* and *gorongosae* sp. nov.), animals classified as *R. gorongosae* sp. nov. and *R. swinnyi* s.s. had short bacula with reduced bases (negative scores on PC1 and PC2), the majority of which presented with a characteristic notch on one side of the shaft tip (position variable). A slightly wider baculum shaft and broader tip (higher PC2 scores) distinguished *R. swinnyi* from *R. gorongosae* sp. nov. The long tapered baculum of *R. rhodesiae* with its broad base (high positive PC1 and PC2 scores), and the shallow notch in the lower shaft visible in lateral profile was clearly distinct from all other specimens in the *swinnyi* complex (Figs 7 and 8). Within *landeri* s.l. (*landeri* and *lobatus*), individuals from Chihalatan Cave and Gorongosa National Park (labelled 1 in Table 5 and Fig. 7) herein referred to as *R. lobatus* had a long, wide baculum, with a spatulate tip and asymmetric base (the dorsal and ventral edges being of different heights). Two individuals of *lobatus* from Mozambique (Pemba and Gorongosa National Park, numbered 2 in Table 5 and Fig 7) have a long, robust baculum with distinctive flanges on the ventral surface and an asymmetric base. On the other hand, the other *lobatus* bacular types (numbered 3-4 in Fig. 7) are smaller and more gracile (Figs 7 and 8). Compared to *R. lobatus*, the Mount Nimba individual (*R. landeri*), had a shorter baculum with a distinctly bulbous tip (Table 5, Figs 7 and 8). Within *R. simulator* s.l., animals from Zimbabwe and South Africa (n = 6), were distinct from specimens originating from Stanhope Mine in South Africa (n = 3), based on their deeper basal notch, spatula-shaped tip and less robust base (Figs 7 and 8).

QUALITATIVE CHARACTERS

Noseleaf morphology. Populations assigned to *Rhinolophus swinnyi* s.l. animals fell into three distinct groups based on anatomical structure of the connecting process and lancet (top row; Fig. 9). *Rhinolophus gorongosae* sp. nov.possessed a subtriangular lancet with straight to slightly concave sides, and a high, rounded connecting

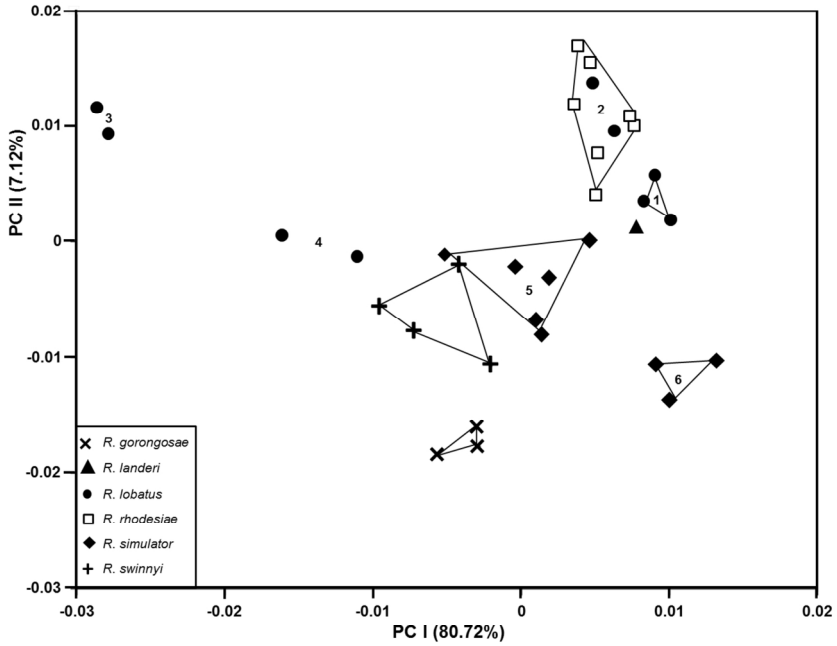

Figure 7. Biplot showing the first and second principal components from a PCA of eight bacular measurements for small southern Africa Rhinolophus taxa. Numbers indicate the position of taxa referred to in Table 5.

169x138mm (300 x 300 DPI)

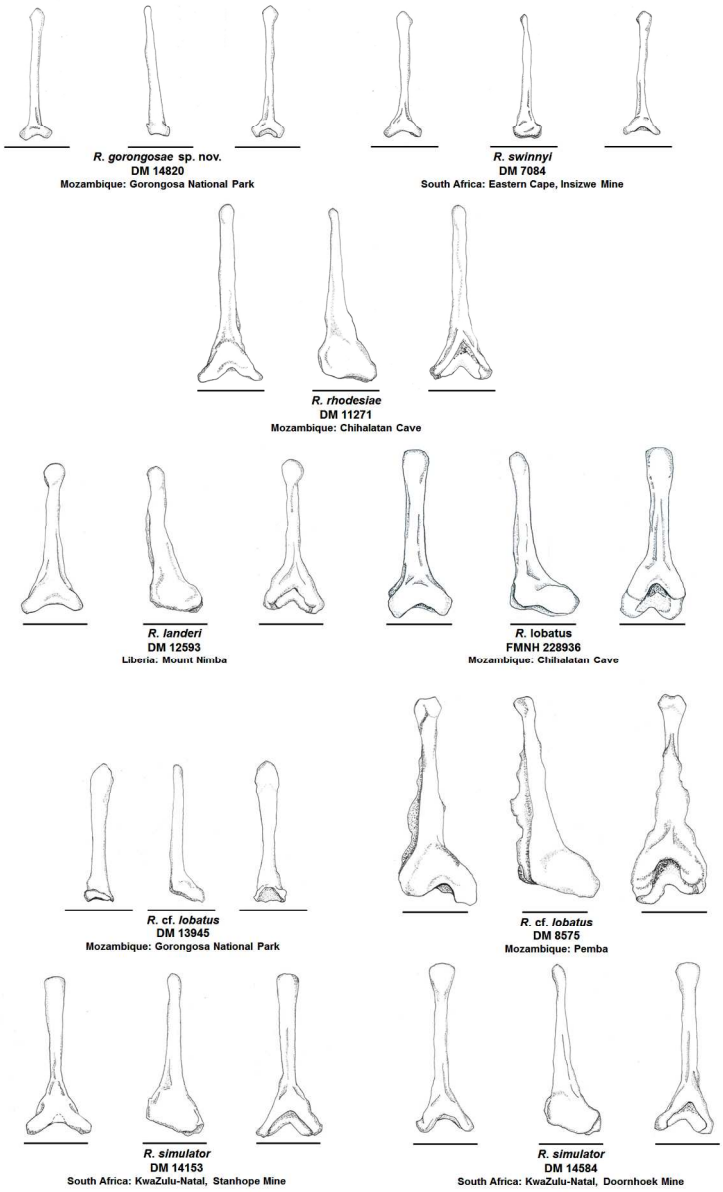

Figure 8. Dorsal, lateral and ventral views (from left to right) of bacula of nine of the 10 taxa as identified by PCA of bacular measurements. Scale bars = 1 mm.

403x652mm (96 x 96 DPI)

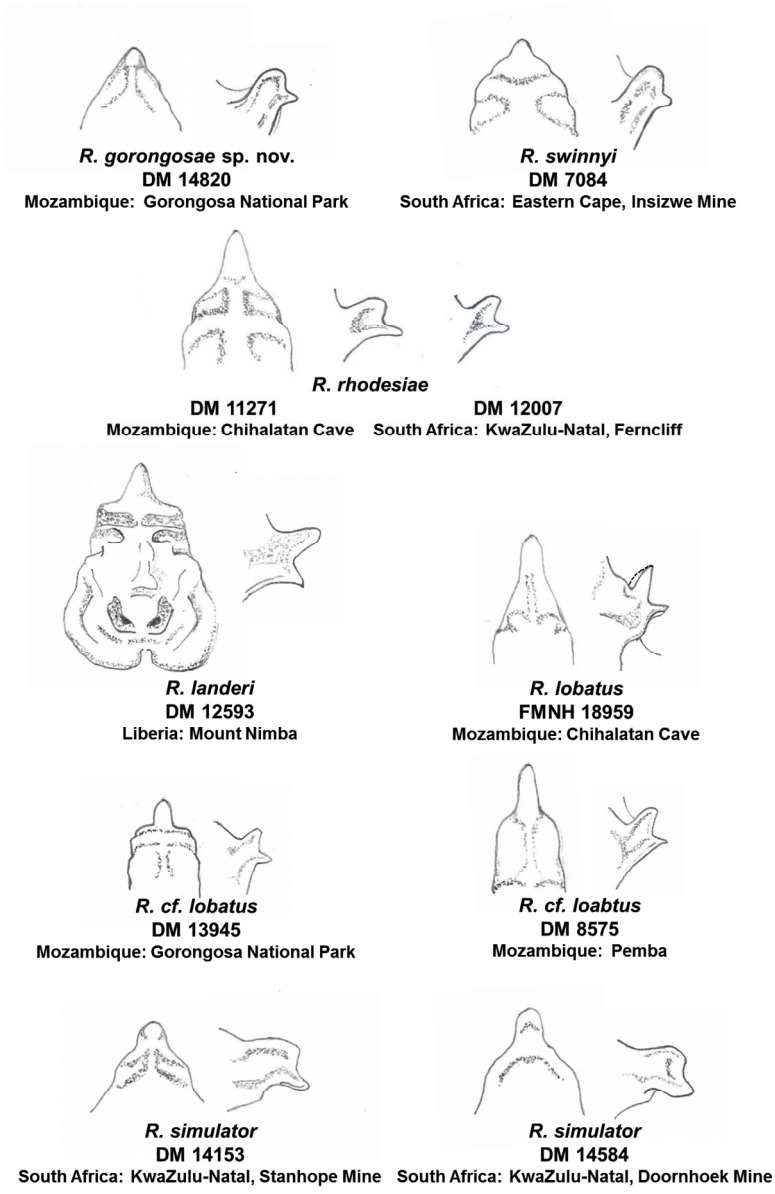

Figure 9. Noseleaf structure of representatives of various Rhinolophus taxa (not drawn to scale).

268x344mm (150 x 150 DPI)

process; the sella has a diminutive, pointed tip. *Rhinolophus swinnyi* s.s. presented with a subtriangular lancet with concave sides and bluntly pointed tip, and a high, rounded connecting process, with a bluntly pointed sella tip directed downwards. *Rhinolophus rhodesiae* was characterised by a hastate lancet and less erect, low rounded, anteriorly projecting connecting process, and pronounced sella tip. *Rhinolophus landeri* from Liberia possessed a short, narrow lancet with a pointed tip, a less erect and subtriangular connecting process, markedly constricted sella and a downward facing sella tip. *Rhinolophus lobatus* had a tall, subtriangular lancet with slightly concave sides and a rounded tip. The connecting process was erect and subtriangular, the sella bore a deep constriction, and the sella tip was sharper and more anteriorly directed than the West African form. Two additional *R. lobatus* forms were documented: one, from Gorongosa National Park, with a small hastate lancet and bluntly pointed tip, and a relatively small subtriangular connecting process with reduced sella tip, and another group from Pemba and Gorongosa National Park (Mozambique) with a tall, hastate lancet, a high, subtriangular (partially rounded) connecting process, and a sharply pointed sella tip (Fig. 9). Animals classified under *R. simulator* s.l. exhibited two distinct morphologies: one with a subtriangular lancet with concave side and a rounded tip, and a low, rounded, wide connecting process, with an asymmetric sella tip, and another with a hastate lancet, pronounced bluntly pointed tip, and a low, rounded, wide connecting process; the sella tip was broader than the other group (Fig. 9).

Dental variation

We observed subtle differences in the size and position of the anterior premolar (PM^1) among the taxa examined above (Fig. 10). *Rhinolophus swinnyi*, *R. gorongosae* sp. nov. and *R. rhodesiae* all possessed a minute and laterally displaced PM^1. The alveolar borders of canine and PM^2 in *R. swinnyi* were almost in contact, whereas in *R. gorongosae* sp. nov. and *R. rhodesiae* a distinct gap was present. The PM^1 in *R. landeri* and *R. lobatus* was positioned in the toothrow and due to its relatively larger size than the afore-mentioned taxa, resulted in a larger space between the canine and PM^2. The anterior premolar of the Pemba individual is more robust than other *lobatus*-type specimens and was positioned further in the toothrow. One of the two *R. simulator* taxa, (as identified by baculum and noseleaf morphology), had a PM^1 situated more external to the toothrow, resulting in a more narrowed space between the alveolar borders of the canine and PM^2, when compared to the other taxon.

ACOUSTIC ANALYSIS

Recent large series obtained in 2007 and 2015 from two adjacent caves (1 km apart) in the Inhambane Province of Mozambique, specifically the Malashane and Chihalatan Caves, comprised both *R. rhodesiae* and *R. lobatus*. Specimens collected from Chihalatan in October 2007 comprised only *R. rhodesiae*, those from February and May

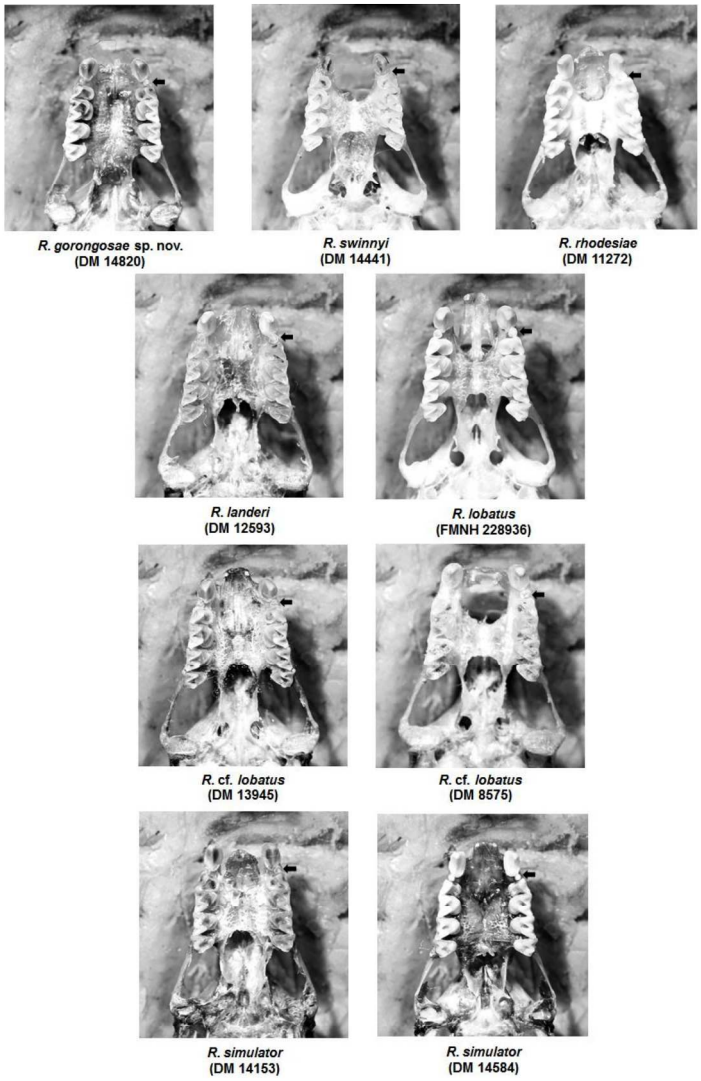

Figure 10. Occlusional views of the maxillary toothrows of the various Rhinolophus taxa detailed in this study. Arrows indicate the position of the small anterior premolar.

264x380mm (300 x 300 DPI)

2015 comprised only *R. lobatus*. The specimens collected in February and May 2015 from Malashane Cave comprised predominantly *R. rhodesiae* with a few individuals of *R. lobatus*. The larger-sized *R. lobatus* from Chihalatan and Malashane Caves had CF frequencies of ca. 107 kHz. The smaller-sized *R. rhodesiae* from Chihalatan and Malashane Caves had CF frequencies of 99–102 kHz, which did not match any known African rhinolophid species (Monadjem *et al.*, 2010). Peak frequencies for Gorongosa National Park *R. gorongosae* sp. nov.

and *R. lobatus* were 103 kHz and 107 kHz, respectively. Maximum frequencies of the two *R. landeri* specimens from Mount Nimba, Liberia, were 104–105 kHz.

DISCUSSION

PHYLOGENY, HYBRIDIZATION AND SPECIATION IN THE *R. SWINNYI* AND *R. LANDERI* COMPLEXES

Although molecular evidence combined with morphological and acoustic characters are powerful diagnostic tools to reveal cryptic species of bats, including African horseshoe bats of the genus *Rhinolophus* (Taylor *et al.*, 2012; Jacobs *et al.*, 2013), a growing body of evidence attests to the frequency of past hybridization events between closely and even distantly related lineages of bats (Artyushin *et al.*, 2011; Nesi *et al.*, 2011; Vallo *et al.*, 2013; Khan, Phillips & Baker, 2014); and pertinently Dool et al. (2016) revealed introgression of *R. ferrumequinum* into *R. clivosus*. Molecular genetic evidence from mtDNA reveals that some morphologically distinct “good” species may be genetically very similar. Such cases of hybridization have been attributed to the past divergences of two species, where after subsequent environmental changes led to the expansion of one species range into that of the other (Artyushin *et al.*, 2011; Vallo *et al.*, 2013). We propose that an analogous scenario may explain the enigmatic genetic affinities recovered for the morphologically distinctive *R. simulator* and *R. rhodesiae*. These two species currently overlap in range (Fig. 1) and are clearly differentiated on craniometric (Figs. 4–6; Table 2), bacular (Figs. 7, 8; Table 5), noseleaf (Fig. 9), dental (Fig. 10) and acoustic (Table 2) evidence. We conclude they are highly unlikely to be recently diverged sister species.

Apart from this single apparent case of historical introgression, taxa within the former *swinnyi* s.l. and *landeri* s.l. complexes are well differentiated from each other based on cyt *b* sequences, 7.2–13.2% between the three taxa within *swinnyi* s.l. and 20.2% between the two taxa within *landeri* s.l. (Table 1). Clearly, cryptic species within both species complexes are paraphyletic (Fig. 2), indicating that the morphological characters used to define these species-groups are subject to convergent evolution. For example, the distinctive erect connecting process and brown apical tufts in males of the *landeri* group clearly evolved independently in *R. lobatus* (which is basal to all other African taxa in our study) and *R. landeri* s.s. which is nested within *R. gorongosae* sp. nov. This

paraphyletic relationship between *R. landeri* from West Africa and *R. gorongosae* from central Mozambique is unlikely to be due to historical introgression given the widely disjunct distributions of these two species and the high genetic distance between them (p = 15%). The range of *R. gorongosae* sp. nov. is still poorly known (awaiting further sampling) but we propose that speciation of this taxon was associated with the establishment of unique habitats on the inselbergs of the Gorongosa range, isolated high above the coastal plain (see Moore, Cotterill & Key, 2017), where it is congruent with the recently described endemic gecko, *Afroedura gorongosa* (Branch *et al*., 2017). The speciation of another recently described cryptic horseshoe bat, *R. mabuensis*, was associated with isolated montane forest patches on inselbergs of northern Mozambique (Mounts Mabu and Inago), and similarly, *R. smithersi* has a distribution that is largely associated with the Soutpansberg and Waterberg ranges in South Africa (Taylor *et al*., 2012). To reinforce this point, a specimen of *R*.cf. *swinnyi* from Mount Inago has a very small size within the range of *R. gorongosae* sp. nov. and, without molecular data, is tentatively assigned to *R. gorongosae* sp. nov.

Known specimens restrict *R. swinnyi* s.s. to the Eastern Cape Province and the southern and central reaches of the KwaZulu-Natal Province, both within South Africa (Fig. 11). *Rhinolophus rhodesiae* occurs from the central and northern regions of the KwaZulu-Natal Province and Limpopo Province, extending northwards to at least Zambia, northern Mozambique and Tanzania (Fig 11). Based on recent collections, *R. gorongosae* sp. nov.is restricted to the Gorongosa Mountains, and possibly Mount Inago. In the case of *R. landeri* s.l., *R. lobatus* seems to occur throughout Mozambique (and probably more widely in southern Africa), while *R. landeri* s.s. occurs in west, central, north and north-eastern Africa (Fig. 11). Due to lack of sampling, the ranges of these respective species and the location of the break between them remain uncertain.

The mechanism(s) of speciation of these cryptic species of *Rhinolophus* are not yet clear. The chronometric tree with dated nodes, estimated in BEAST from six nuclear introns (Figure S5 in Dool *et al*., 2016), constrains the formative nodes that shaped diversification of Afrotropical *Rhinolophus* to the late Neogene; the founding of the clade including *simulator* s.s. and *swinnyi* s.s. lineages is constrained to 4.89 (6.61 – 3.5) Mya, with the *alcyone* and *landeri* complexes at 4.42 (6.41 - 2.85) Mya. Following Dool et al (2016) divergence of *R. swinnyi* s.s. from other lineages of the *capensis*-group (including both *simulator* and *rhodesiae*, classified by them as “cf. *simulator*”) is estimated at ~2.5 Mya; with isolation of *R. simulator* and *R.* cf. *simulator* (= *rhodesiae*) estimated as Early Pleistocene (~2 Mya), but the latter estimate might be biased by historical introgression as discussed above.

The recurrent uplift and volcanism along the Albertine Rift System has been invoked to explain allopatric speciation in large and small mammals, and centred on the ``Mbeya triple junction'' and Rungwe volcanic province between lakes Malawi and Rukwa (Cotterill, 2003; Faulkes *et al*., 2011, 2017). Recurrent uplift of southern Africa (intensifying erosion) acted to accentuate the relief along the eastern lowlands from the central Plateau and

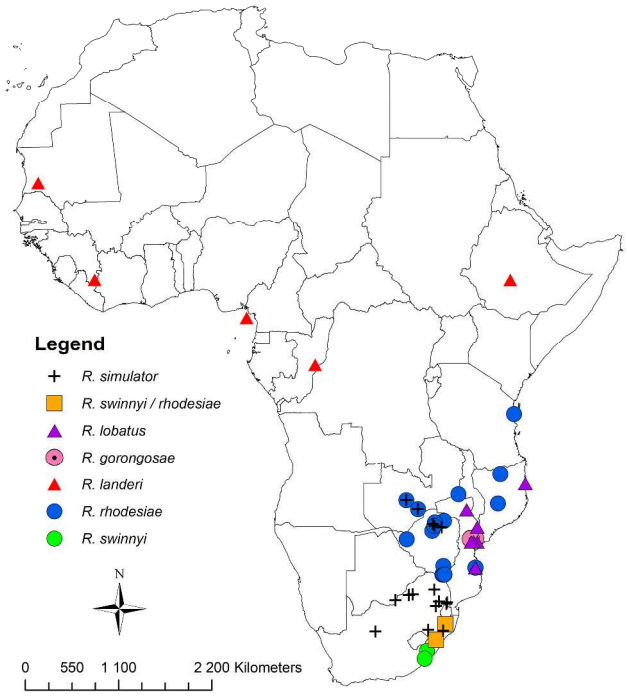

Figure 11. Final distribution of small Rhinolophus species classified according to the present study.

296x419mm (300 x 300 DPI)

Eastern Highlands of Zimbabwe to the Eastern Cape (Partridge 1998; Partridge & Maud, 2000; Moore *et al*. 2009). These twinned geomorphic processes are also invoked to have isolated Mount Gorongosa and neighbouring inselbergs in Central Mozambique (Moore, Cotterill & Key, 2017). It is possible that these regional palaeoclimatic and geomorphological events acted in concert to cause the allopatric speciation of horseshoe bats within the *landeri* s.l. and *swinnyi* s.l. complexes. Further phylogeographic studies informed by broader sampling are required to unravel the causes of the evolution of these two species complexes.

TAXONOMIC CONCLUSIONS

DESCRIPTION AND RE-DEFINITION OF SPECIES

FAMILY RHINOLOPHIDAE BELL, 1836

GENUS RHINOLOPHUS LACÉPÈDE 1799

***RHINOLOPHUS GORONGOSAE* SP. NOV.**

LEAST HORSESHOE BAT

Holotype: Durban Natural Science Museum (DM) No. 14820 (field number JAG196), is an adult male, preserved in 70% ethyl alcohol, originally part of series of specimens collected by J. A. Guyton on 25 April 2015. The cranium and baculum has been extracted and examined for this study. The specimen has been included in both morphometric analyses.

Type locality: Bunga Inselberg, Gorongosa National Park, Sofala Province, Mozambique -18.599° S, 34.343° E, 212 m.

Paratypes: Eight specimens collected 24–25 April 2015 (DM 14815–14819), 2 May 2015 (DM 14828), 5 November 2015 (DM 14843) and 22 July 2015 (DM 14865).

Referred specimens having molecular identification: DM 14815 (JAG 188) a female specimen collected by J. A. Guyton from Mozambique, Sofala Province, Gorongosa National Park, Bunga Inselberg, -18.599° S, 34.343° E, 212 m; DM 14843 (JAG 228) a female specimen collected by J. A. Guyton from Mozambique, Sofala Province, Gorongosa National Park, -18.694° S, 34.208° E, 308 m.

Referred specimens having only morphological identification: TMSA 49116 (JAG 31), adult male, collected on 21 April 2013 by J. A. Guyton from Mozambique, Sofala Province, Gorongosa National Park, Cheringoma Plateau, Gorge Rim, Site 1, -18.635° S, 34.808° E, 213 m. *Incertae sedis*: DM 14864 adult female collected by J. A. Guyton on 21 July 2015 from Mozambique, Sofala Province, Gorongosa National Park, -18.465° S, 34.052° E, 1150 m; DM 11482, adult female collected on 1 May 2009 by J. Bayliss from Mozambique, Nampula Province, Mount Inago Forest Camp, -15.045° S, 37.396° E 1478 m.

Etymology: The species derives its name from the Gorongosa district of Mozambique, in particular Gorongosa National Park, a biologically diverse region of southern Africa.

Diagnosis: The species can be clearly distinguished from both *R. swinnyi* s.s. and *R. rhodesiae* on molecular grounds (Figs. 2 and 3) as well as by its smaller size (Fig. 4, Table 2), distinct cranial shape (Figs. 5 and 6), echolocation call peak frequency (Table 2), baculum (Figs. 7 and 8) and noseleaf (Figs. 9, 12) characteristics. Although some measurements overlap, there is minimal overlap in condylocanine skull length and zygomatic skull width between this species (14.8–15.2 mm; 8.13–8.56 mm) and *R. swinnyi* (14.3–16.0 mm; 8.7–9.2 mm) and *R. rhodesiae* (15.1–15.7; 8.46–8.96 mm). The small size of this form makes it even smaller than *denti* (regarded by Csorba *et al*., 2003 as the smallest species in the Ethiopian region), therefore making this new species Africa's smallest horseshoe bat. Comparing means for *R. gorongosae* sp. nov. (Table 2) and *denti* (Monadjem *et al*., 2010): forearm 41.3 mm cf. 43.1 mm; mass 5.6 g cf. 7.0 g.

Description: The genetically-distinct *R. gorongosae* sp. nov. is similar in pelage colour but distinctly smaller in external (mean total length 68 mm, mean forearm length = 41 mm) and cranial (mean condylocanine length 15.1 mm) measurements (Table 2) than both *rhodesiae* (mean total length 75 mm, forearm length 44 mm, condyolocanine length 15.4 mm) and *swinnyi s.s.* from South Africa (mean total length 73 mm, forearm length 44 mm, condyolocanine length 15.4 mm). Based on geometric morphometric results, the diminutive *R. gorongosae* sp. nov. has a reduced foramen magnum, a noticeable depression along the parietal region, low set bullae, a narrow braincase and a narrow and high set nasal inflation with a sharp slope from the nasal inflation to the maxillae (Fig. 6). Lancet is subtriangular with straight to slightly concave sides, and a high, rounded connecting process; the sella has a diminutive, pointed tip (Fig. 12). Baculum short with reduced base, with a characteristic notch on one side of the shaft tip (position variable). The slightly narrower baculum shaft with narrower tip distinguishes *R. gorongosae* sp. nov. from *R. swinnyi* (Table 5, Figs 7 and 8). Maxillary toothrow with minute and

Figure 12. Portraits of a) the lateral facial profile showing the connecting process, b) general noseleaf morphology and c) in flight behaviour of Rhinolophus gorongosae sp. nov. (Photographs by P. Naskrecki).

262x328mm (300 x 300 DPI)

laterally displaced PM^1 with a distinct gap between the alveolar borders of canine and PM^2 (Fig. 10). Mean peak echolocation CF frequency is 106 kHz (104–108 kHz; Table 2).

Distribution and biology: So far, it appears that this tiny species is restricted in its distribution to Gorongosa National Park in Mozambique (Fig. 11), although we provisionally refer a very small adult individual from Mount Inago in Mozambique to this taxon. Molecular sequences are required from a wider range of localities to determine the range of this taxon. Given that the two individuals sequenced from Gorongosa National Park were distinct from each other, the possibility exists that more than one cryptic species may be present.

RHINOLOPHUS RHODESIAE ROBERTS, 1946

ROBERTS'S HORSESHOE BAT

Synonyms: None

Holotype: TMSA 1325, adult female, collected by A. Roberts on 16 August 1913.

Type locality: "Southern Rhodesia" (= Zimbabwe), Bezwe River, tributary of "Wanetsi" (=Nuanetsi) River, -21.500˚S, 31.167˚ E.

Referred specimens having molecular identifications: FMNH 228942 (SMG 19017), female, 228943 (SMG 19018), male, 228944 (SMG 19019), female, 228945 (SMG 19020), male, 228946 (SMG 19021), female, 228948 (SMG 19023), male, 228949 (SMG 19024), female, 228950 (SMG 19025), female, 228951 (SMG 19026), female, 228952 (SMG 19027), male, 228953 (SMG 19028), male, 228955 (SMG 19030), male, 228957 (SMG 19032), female, 228958 (SMG 19033), female, 228959 (SMG 19034), female, 228960 (SMG 19035), female, 228961 (SMG 19036), male, 228962 (SMG 19037), male, 228964 (SMG 19039), female, all collected on 2 May 2015 by S. M. Goodman, M. C. Schoeman and G. le Minter from Mozambique, Inhambane Province, Malashane Cave, 39.1 km Efrom Inhassoro, -21,668˚S, 34,847˚E, and situated < 2 km from Chihalatan Cave referred to above.

Referred specimens having only morphological identifications: DM 7080, adult male, KwaZulu-Natal Province, Hlabeni Forest Reserve, -29.933° S, 29.766° E collected by D. Forbes on 29 July 2000; DM 12007 (adult male); DM 14034 (adult male), collected by M. C. Schoeman from KwaZulu-Natal Province, Pietermaritzburg, Ferncliff Nature Reserve, Ferncliff Cave, -29.550 ° S, 30.320° E; DM 11270 (female), 11271 (male), 11272 (female), 11273 (female), 11275 (male), all collected by S. Stoffberg from Chihalatan Cave, 38.2 km E of Inhassoro, Inhambane

Province, Mozambique -21.671˚S, 34.864˚E;. DM 11275 collected on 8 August 2006 while the other specimens were collected on 3 September 2007; FMNH 228956 (SMG 19031), collected 2 May 2015 by S. M. Goodman, M. C. Schoeman and G. le Minter from Mozambique, Inhambane Province, Malashane Cave, km 39.1 E from Inhassoro, -21,668˚S, 34,847˚E; DM 13450 (female), DM13451 (female), collected on 8 May 2012 by J. Bayliss at Mozambique, Niassa Province, Mount Mecula, -12.068° S, 37.662° E.

Etymology: The name refers to the location in Southern Rhodesia (now Zimbabwe) where the type specimen was collected.

Re-diagnosis and description: Roberts (1946) described this subspecies as being slightly smaller than the nominate *R. s. swinnyi* based on slightly smaller body size, slightly longer tail, smaller ears and its bright ochraceous colour. Since the last-mentioned character is known to be an environmentally induced effect in many cave-dwelling bat species, it does not serve as a diagnostic character. In our analysis, molecular evidence closely matched our series from Chihalatan and Malashane Caves with Genbank sequences from the extreme northern South Africa (Pafuri), Zimbabwe (Dambanzara) and Zambia (Kalenda and Shimalala Caves). Since these localities encompass the type locality of *rhodesiae* (Bezwe River in Zimbabwe), and Pafuri is only 100 km south of Bezwe, we are confident to use this available name for this widespread taxon. The species can be further diagnosed by having echolocation peak frequencies around 100 kHz (99–102 kHz, n = 8 from Malashane Cave; Table 2), which are quite distinct from typical *swinnyi* (105–107kHz, n = 6; Table 2) as well as the new Gorongosa National Park taxon *R. gorongosae* sp. nov. (104–108 kHz, n = 16; Table 2). Noseleaf structure is distinctive, being characterised by a hastate lancet, not as concave as true *swinnyi*, less erect low rounded connecting process and more pronounced posterior lobe. Bacular structure of *rhodesiae* is clearly distinct from other *swinnyi*-like animals (see Figs. 7 and 8), being characterised by a distinctly longer tapered baculum with a distinctly broader base and shallow notch along the lower portion of the shaft that is visible in the lateral profile. Traditional morphometrics (Table 2, Fig. 4) do not differentiate *rhodesiae* from *swinnyi* proper; however, *rhodesiae* is clearly distinguished with minimal overlap from the distinctly smaller *gorongosae* sp. nov. Although quite small, the *R. rhodesiae* holotype falls within the range of variation of specimens assigned to *R. rhodesiae* from Mozambique, Zimbabwe, Zambia, northern South Africa (Pafuri, Limpopo Province), and Zanzibar (Table 2, Fig. 4). It falls clearly outside (larger than) the range of variation of the smaller *gorongosae* sp. nov. taxon (Fig. 4). Geometric morphometric results result in a better separation between *rhodesiae* and *swinnyi* s.s. with only minimal overlap (Fig. 5). Once again, the *rhodesiae* holotype from Bezwe River clusters within the range of variation of the *rhodesiae* taxon and outside the *gorongosae* sp. nov. or *swinnyi* taxa, thus validating the use of this name for this taxon.

Distribution and biology: Combined molecular and morphometric data suggest the widespread distribution of this taxon from central and northern South Africa through Zimbabwe, Zambia and Mozambique extending to Zanzibar (Fig. 11). Based on specimen assignments on morphological grounds, the species co-occurs with *R. swinnyi* in central KwaZulu-Natal at Ferncliff Cave, as well as occurring in close proximity in northern KwaZulu-Natal, recorded at Hlabisi Forest close to Ngome Forest where *swinnyi* was recorded (Fig. 11). The widespread extent of this taxon and its occurrence in northern South Africa is confirmed by the widespread occurrence of a hitherto unidentified 100 kHz acoustic type recorded in the Soutpansberg (Taylor *et al.*, 2013), and Pafuri Region of northern Kruger National Park (Taylor & Parker, unpublished data).

RHINOLOPHUS LOBATUS PETERS, 1852

PETERS'S HORSESHOE BAT

Synonyms: R. l. angolensis (Seabra, 1898), Angola, Hahna.

Type locality: Mozambique, Tete (= Tete Province), Sena village, south bank of the Zambesi River, -15.679° S, 33.809° E.

Syntypes: ZMB 375 (female, poor skin only), ZMB 2496 (female, skin in alcohol, skull extracted, broken), ZMB 24922 (adult male, complete skeleton), ZMB 24927 (female, complete skeleton), collected between 1843 and 1847 by W. C. H. Peters from Mozambique, Tette (=Tete Province), Sena on the south bank of the Zambesi River, -15.679° S, 33.809° E.

Referred specimens having molecular identifications: FMNH 228936 (SMG 18959), male, 228937 (SMG 18988), female, 228938 (SMG 18989), male, 228939 (SMG 18990), male, 228940 (SMG 18991), female, 228941 (SMG 18992), male, all collected on 2 May 2015 by S. M. Goodman, M. C. Schoeman and G. le Minter from Mozambique, Chihalatan Cave, 38.2 km E of Inhassoro, -21,671˚S, 34,864˚E. FMNH: 228947 (SMG 19022), female, 228954 (SMG 19029), female, 228965 (SMG 19040), female, all collected on 2 May 2015 by S. M. Goodman, M. C. Schoeman and G. le Minter from Mozambique, Mozambique, Inhambane Province, Malashane Cave, 39.1 km E of Inhassoro, -21,668˚S, 34,847˚E, and situated < 2 km from Chihalatan Cave referred to above. DM13905 (female), 13916 (female), DM 14531 (male), all collected by A. Monadjem, G. le Minter and E. Lagadec in July 2015 from Mozambique, Sofala Province, Gorongosa National Park.

Referred specimens having non-molecular identifications

DM 13894 (female), 13927 (male), 13938 (unknown sex), 13942 (unknown sex), 13943 (unknown sex), 13944 (unknown sex), 13945 (male), 14529 (male), 14531 (male), 14532 (female), collected by A. Monadjem, G. le Minter and E. Lagadec in July 2015 from Mozambique, Sofala Province, Gorongosa National Park. TMSA 49114 (female), TMSA 49117 (male), collected from Mozambique, Sofala Province, Gorongosa National Park by A. J. Guyton in July 2015 from Chitengo Camp and Cheringoma Plateau respectively. TMSA 14653 (female), 14655 (unknown sex), 14656 (female), 14657 (female), 14662 (male), 14663 (male), 14664 (female), collected 28 – 29 July 1964 from Mozambique, Tete Province, Muchena, -15.679° S, 33.809° E. *Incertae sedis*: DM 8575 (male) from Mozambique, Cabo Delgado Province, Pemba Island (-13.006° S, 40.524° E) and DM 8574 (female), from Mozambique, Sofala Province, Chinizuia Forest (-18.977° S, 35.052° E), both collected by A. Monadjem in June 2006. TMSA 49115 (male), TMSA 49118 (male), collected from Mozambique, Sofala Province, Gorongosa National Park by A. J. Guyton in July 2015 from Chitengo Camp and Cheringoma Plateau respectively.

Etymology: The Latin word *lobatus* means lobed, perhaps referring to the general shape of the noseleaf (See Figure 13).

Re-diagnosis & comparisons: This taxon is clearly phylogenetically distinct on cyt *b* gene sequences (see also Dool *et al.*, 2016) from topotypic *landeri* from West Africa and seems to be more closely affiliated with the *capensis* group of Csorba *et al.* (2003), i.e. *R. capensis*, *R. denti*, *R. simulator* and *R. swinnyi* (Fig. 2). Specimens from Chihalatan and Malashane (n = 4) had a mean echolocation call peak frequency of 106.8 ± 0.4 kHz (Table 2), close to the 107 kHz generally reported for southern Africa "*landeri*" (Monadjem *et al.*, 2010). This contrasts with a mean maximum frequency of 104.3 ± 0.42 kHz (n = 2) recorded for topotypic West African (Liberian) *R. landeri*, making peak frequency of c. 107 kHz a possible diagnostic criterion for *R. lobatus*. However, a wider range (102–108 kHz) and slightly lower mean frequency of 105 kHz was reported for 20 individuals at Gorongosa (Table 2). This variation could be indicative of further undetected cryptic speciation in this taxon, as also indicated by the very wide variation in baculum and noseleaf characters discussed below.

Although not easily distinguished on body or skull size (Table 2, Fig. 4), this taxon differs from topotypic *R. landeri* by displaying a prognathic rostrum (LMs 1–3), a shortened braincase that extends posteriorly (LMs 10–14), and a broader nasal inflation (LMs 16–18) (Figs. 5 and 6). Specimens of cf*. lobatus* from Pemba (Mozambique) had a shorter foramen magnum (LMs 9–10), a narrower jugal process (LM 3–4), and a slightly broader nasal inflation (LMs 16–18), than other Mozambique animals. The same individual from Pemba possessed a distinctive

robust baculum (Fig. 8) and noseleaf (Fig. 9) having a markedly hastate lancet and pronounced posterior lobe of the connecting process. However, pending molecular data, we here refer them to *lobatus incertae sedis*. Although genetically clearly assigned to *lobatus*, individuals from Gorongosa National Park are somewhat smaller in external (but not cranial) measurements (Table 2) and also display unique noseleaf and bacular morphologies. The noseleaf of a Gorongosa individual has a small hastate lancet and bluntly pointed tip, and a relatively small and more erect connecting process with semi-symmetrical lobe (Figs 9, 13), while its baculum is highly divergent from all other forms considered in our study (Fig. 8), having a remarkable short baculum with wide shaft and very small base compared with *landeri* from West Africa and well as cf*. lobatus* from Malashane and Chihalatan Caves. Given the clear evidence for close genetic identity in our study between Malashane and Chihalatan Caves and Gorongosa National Park for animals referred to *R*. *lobatus*, we provisionally regard this variation in noseleaf and baculum structure to represent polymorphic traits in this species. It is possible that these morphological types represent good species between which introgression has occurred. Further analysis with additional nuclear sequences is necessary to test this hypothesis. There is also the possibility that these could represent subadults with bacula that are not fully ossified as detailed in *R. adami* described by Kock *et al.* (2000).

Male *R. lobatus* from Chihalatan and Malashane Caves, as well as Gorongosa National Park, typically possessed a dark brown apical tuft of stiff hairs characteristic of *R*. *landeri* (Fig. 14; Csorba *et al.*, 2003; Monadjem *et al.*, 2010). This convergent character could be one of the contributing factors that have led to the historical misidentification of the species with *R*. *landeri*.

Distribution and biology: As anticipated by Monadjem *et al.* (2010), who considered that the southern (and possibly eastern) African savannah-occurring *lobatus* might prove to be distinct from the West African forest-occurring *landeri*, we here refer all southern African specimens to *lobatus* (Fig. 11; see Appendix of Monadjem *et al.*, 2010 for a full list of localities). We agree with Monadjem *et al.* (2010) that *R. angolensis* Seabra, 1989 from western Angola may merit specific status. Nevertheless, in the absence of the type series that was destroyed in the Lisbon fire of 1978, resolution of its status must await a detailed revision including molecular evidence with designation of new type material. Likewise, the status of east and central African populations must await further studies including molecular data. Until further evidence becomes available, we suggest that it is prudent to use the name *lobatus* for all savannah populations in southern and east Africa.

RHINOLOPHUS SWINNYI GOUGH, 1908

SWINNY'S HORSESHOE BAT

Figure 13. Portraits of a) the lateral facial profile showing the connecting process, b) general noseleaf morphology and c) in flight behaviour of Rhinolophus lobatus. (Photographs by P. Naskrecki).

256x314mm (300 x 300 DPI)

Figure 14. Colony of R. lobatus showing present of orange apical tuft in flying males (Photographs by P. Naskrecki).

151x109mm (300 x 300 DPI)

Synonyms: Rhinolophus swinnyi piriensis Hewitt, 1913, South Africa, Eastern Cape Province, Pirie, near King Williams Town.

Types: TMSA 1021 (holotype, male), 1022 (cotype, male), collected on 22-23 February 1908 by H. H. Swinny.

Type locality: South Africa, Eastern Cape Province, Pondoland, Ngqeleni District, -31.667° S, 29,033° E.
Referred specimens having molecular identifications: None

Referred specimens having only morphological identifications: All specimens originate from South Africa. DM: 7084, adult male collected by P. J. Taylor on 3 March 2001 and DM 13250, 13252 and13254 (all of unknown sex), collected by E. J. Richardson on 2 November 2010 from the Eastern Cape Province, Insizwe Mine, (-30.804° S, 29.281° E); DM 14036 (male), collected by M.C. Schoeman on 9 May 2012 from the KwaZulu-Natal Province, Pietermaritzburg, Ferncliff Nature Reserve, (-29.550° S, 30.320° E); DM 14291 (female),and 14292 (female) collected by L. R. Richards on 1 April 2014 from the KwaZulu-Natal Province, Eshowe, Entumeni Nature Reserve, (-28.886° S, 31.376° E); DM 14441 (female), and14440 (male), collected by S. Stoffberg and M. C. Schoeman on 23 July 2004 from Eastern Cape Province, Kokstad Mine, (-30.810° S, 29.280° E); DM 15018, adult female, collected by L. R. Richards on 7 April 2016 from Eastern Cape Province, Sandile's Rest Trout and Forest Country Estate, (-32.661° S, 27.298° E); TMSA 39848, adult male collected by G. Bronner on 14 March 1988, from KwaZulu-Natal Province, Ngome Forest Reserve, (-27.833° S, 31.413° E).

Re-diagnosis & comparisons: Gough's (1908) original description emphasized *inter alia*, the very small size of the species, the "mouse=grey" colour, the position of the anterior premolar within the toothrow, the medium-sized ears, the shape of the connecting process ("forming a marked projection, rounded terminally"), the parallel-sided edges of the sella, and the moderate lancet with strongly concave edges. *Rhinolopus swinny* s.s., as defined here, confined to the Eastern Cape, KwaZulu-Natal and possibly Mpumalanga Provinces, South Africa, is clearly distinct on molecular grounds from *R. rhodesiae* and *R. gorongosae* sp. nov., and has as its closest relative, *R. capensis* with which it overlaps in range in the Eastern Cape. The echolocation peak frequency of *R. swinnyi s.s.* calls recorded in the Eastern Cape (mean 106.6 ± 0.4 kHz, n = 10, Schoeman & Jacobs, 2008) and KwaZulu-Natal (mean 105,6 ± 0.76 kHz; this study) Provinces, South Africa overlap considerably, but differ clearly from the 100 kHz calls of *R. rhodesiae* from central and northern South Africa and Mozambique (and probably more broadly).

Although *R. swinnyi* s.s. overlaps in external and cranial characters with *R. rhodesiae*, it can be distinguished from the latter taxon based on both baculum and noseleaf characters, as well as on detailed cranial

shape analysis (see above). It can be differentiated from *R. gorongosae* sp. nov. on its larger size (e.g. condyle-canine skull length 14.8–15.2 mm in *R. gorongosae* sp. nov., 14.3–16.0 mm in *R. swinnyi*; zygomatic width 8.13–8.56 mm in *R. gorongosae* sp. nov., 8.7–9.2 mm in *R. swinnyi*; Table 2), as well as on noseleaf, bacular and subtle cranial shape characters (see above).

Distribution and biology: We here restrict the distribution of *R. swinnyi* s.s. to South Africa, including the Eastern Cape and KwaZulu-Natal Provinces and possibly Mpumalanga Province (Fig. 11). However, a recent specimen collected from the montane western region of Swaziland has tentatively been assigned to *R. rhodesiae* based on morphology and acoustics (maximum frequency = 102 kHz), but a molecular analysis has yet to be conducted (A. Monadjem, unpublished data); this suggests that *R. rhodesiae* (and not *R. swinnyi*) occurs to the north in Mpumalanga Province. Specimens from Limpopo Province in the north of South Africa are referred to *R. rhodesiae*. As pointed out above, *swinnyi* and *rhodesiae* co-occur at at least one locality, Ferncliff Cave, in central KwaZulu-Natal.

ACKNOWLEDGEMENTS

We thank Prof. Christiane Denys for access to the collections of the Muséum National d'Histoire Naturelle in Paris, and Dr Frieder Mayer for access to the Zoologisches Museum in Berlin. Julian Bayliss provided specimens from Mount Mecula, Mount Mabu and Mount Inago in Mozambique. Two field trips to the Inhassoro District of Mozambique in 2015 were financed by a grant from FEDER, under the name POCT MOZAR, to Centre de Veille sur les maladies émergentes en Océan Indien (CRVOI). Gildas le Minter, Erwan Lagadec and Charles Gumbi are thanked for help with fieldwork in Mozambique. PJT acknowledges the financial support of the University of Venda, the South African National Research Foundation and the Department of Science and Technology under the South African Research Chair Initiative (SARChI) on Biodiversity Value and Change within the Vhembe Biosphere Reserve hosted at University of Venda and co-hosted by the Centre for Invasion Biology at University of Stellenbosch. For assistance with obtaining research and shipping permits we acknowledge Gorongosa National Park, Department of Scientific Services; Universidade Eduardo Mondlane, Museu de História Natural; South African Department of Agriculture, Forestry and Fisheries, and eZemvelo KZN Wildlife.

REFERENCES

African Chiroptera Report. 2015. *African Chiroptera Report. 2015.* Pretoria: African Bats.

Artyushin IV, Bannikova AA, Lebedev VS, Kruskop SV. 2009. Mitochondrial DNA relationships among North Palaearctic *Eptesicus* (Vespertilionidae, Chiroptera) and past hybridization between Common Serotine and Northern Bat. *Zootaxa* **2262:** 40–52.

Bandelt H, Forster P, Röhl A. 1999. Median-joining networks for inferring intraspecific phylogenies. *Molecular Biology and Evolution* **16:** 37–48.

Benda P, Vallo P. 2012. New look on the geographical variation in *Rhinolophus clivosus* with description of a new horseshoe bat species from Cyrenaica, Libya. *Vespertilio* **16:** 69–596.

Brooks DM, Bickham JW. 2014. New species of *Scotophilus* (Chiroptera: Vespertilionidae) from Sub-Saharan Africa. *Occasional Papers of the Museum, Texas Tech University* **326:** 1–21.

Branch WR, Guyton JA, Schmitz A, Barej MF, Naskrecki P, Farooq H, Verburgt L, Roedel MO. 2017. Description of a new flat gecko (Squamata: Gekkonidae: *Afroedura*) from Mount Gorongosa, Mozambique. *Zootaxa* **4324:**142-60.

Cotterill FPD. 2002. A new species of horseshoe bat (Microchiroptera: Rhinolophidae) from south-central Africa: with comments on its affinities and evolution, and the characterization of rhinolophid species. *Journal of Zoology London* **256:**165-179.

Cotterill FPD. 2003. Geomorphological influences on vicariant evolution in some African mammals in the Zambezi basin: some lessons for conservation. In: A. Plowman. (Ed.) *Ecology and Conservation of Small Antelope. Proceedings of an International Symposium on Duiker and Dwarf Antelope in Africa*. Filander Verlag, Fürth. pp 11-58.

Cotterill FPD. 2013. *Rhinolophus swinnyi*. In: Happold M, Happold DCD, eds. *Mammals of Africa*. *Volume IV: Hedgehogs*, *Shrews and Bats*. pp. 353-355. London: Bloomsbury Publishing.

Csorba G, Ujhelyip P, Thomas N. 2003. Horseshoe Bats of the World (Chiroptera: Rhinolophidae). Shropshire: Alana books.

Darriba D, Taboada GL, Doallo R, Posada D. 2012. jModelTest 2: more models, new heuristics and parallel computing. *Nature Methods* **9:** 772.

Decher J, Hoffmann A, Schaer J, Norris RW, Kadjo B, Astrin J, Monadjem A, Hutterer R. 2015. Bat diversity in the Simandou Mountain Range of Guinea, with the description of a new white-winged vespertilionid. *Acta Chiropterologica* **17:** 255–282.

Dool SE, Puechmaille SJ, Foley NM, Allegrini B, Bastian A, Mutumi GL, Maluleke TG, Odendaal LJ, Teeling EC, Jacobs DS. 2016. Nuclear introns outperform mitochondrial DNA in inter-specific phylogenetic reconstruction: Lessons from horseshoe bats (Rhinolophidae: Chiroptera). *Molecular Phylogenetics and Evolution* **97:**196–212.

Ellerman JR, Morrison-Scott TCS Hayman RW. 1953. Southern African Mammals 1758–1951: A Reclassification. London: British Museum (Natural History).

Faulkes CG, Bennett NC, Cotterill FPD,Stanley W, Mgode GF, Verheyen E. 2011. Phylogeography and cryptic diversity of the solitary-dwelling silvery mole-rat, genus *Heliophobius* (family: Bathyergidae). *Journal of Zoology* **285:324–338** DOI: 10.13140/2.1.1922.6566

Faulkes CG, Mgode GF, Archer EK, Bennett NC. 2017. Relic populations of *Fukomys* mole-rats in Tanzania: description of two new species *F. livingstoni* sp. nov. and *F. hanangensis* sp. nov. *PeerJ.* **27:** 5:e3214.

Fahr J, Vierhaus R, Hutterer R, Kock D. 2002. A revision of the *Rhinolophus maclaudi* group with the description of a new species from West Africa (Chiroptera: Rhinolophidae). *Myotis* **40**: 95–126.

Goodman SM, Bradman HM, Maminirina CP, Ryan KE, Christidis LL, Appleton B. 2008. A new species of *Miniopterus* (Chiroptera: Miniopteridae) from lowland southeastern Madagascar. *Mammalian Biology-Zeitschrift für Säugetierkunde* **73**:199–213.

Goodman SM, Buccas W, Naidoo T, Ratrimomanarivo F, Taylor PJ, Lamb J. 2010. Patterns of morphological and genetic variation in western Indian Ocean members of the *Chaerephon* '*pumilus*' complex (Chiroptera: Molossidae), with the description of a new species from Madagascar. *Zootaxa* **2551**: 1–36.

Goodman SM, Ramasindrazana B, Maminirina CP, Schoeman MC, Appleton B. 2011. Morphological, bioacoustical, and genetic variation in *Miniopterus* bats from eastern Madagascar, with the description of a new species. *Zootaxa* **17**: 2880:1–9.

Goodman SM., Schoeman MC, Rakotoarivelo AR, and Willows-Munro S. 2016. How many species of *Hipposideros* have occurred on Madagascar since the Late Pleistocene? *Zoological Journal of the Linnean Society* **177**: 428–449.

Goodman SM, Kearney T, Ratsimbazafy MM, Hassanin A. 2017. Description of a new species of *Neoromicia* (Chiroptera: Vespertilionidae) from southern Africa: A name for "*N.* cf. *melckorum*". *Zootaxa* **4236:** 4232–4210.

Guindon S, Gascuel O. 2003. A simple, fast and accurate method to estimate large phylogenies by maximum-likelihood. *Systematic Biology* **52**: 696–704.

Hall TA. 1999. *BioEdit* A User-Friendly Biological Sequence Alignment Editor and Analysis Program for Windows 95/98/NT. *Nucleic Acids Symposium Series* **41**: 95–98.

Hammer O, Harper DAT, Ryan PD. 2001. Paleontological Statistics software package for education and data analysis. *Palaeontologia Electronica* **4:** 1–9.

Happold M, Cotterill FPD. 2013. Family Rhinolophidae Horseshoe Bats. In: Happold M, Happold DCD, eds. *Mammals of Africa. Volume IV: Hedgehogs*, *Shrews and Bats*. pp. 300–309. London: Bloomsbury Publishing.

Hassanin A, Khouider S, Gembu GC, Goodman SM, Kadjo B, Nesi N, Pourrut X, Nakoune E, Bonillo C. 2015. The comparative phylogeography of fruit bats of the tribe Scotonycterini (Chiroptera, Pteropodidae) reveals cryptic species diversity related to African Pleistocene forest refugia. *Comptes Rendus Biologies* **338:** 197–211.

Hassanin A, Colombo R, Gembu G-C, Merle M, Tu VT, Görföl T, Akawa PM, Csorba G, Kearney T, Monadjem A, Ing RK. 2017. Multilocus phylogeny and species delimitation within the genus *Glauconycteris* (Chiroptera, Vespertilionidae), with the description of a new bat species from the Tshopo Province of the Democratic Republic of the Congo. *Journal of Zoological Systematics and Evolutionary Research*: 2017;00:1–22. https://doi.org/10.1111/jzs.12176

Hill JE, Harrison DL. 1987. The baculum in the Vespertilionidae (Chiroptera:Vespertilionidae) with a systematic review, a synopsis of *Pipistrellus* and *Eptesicus*, and the descriptions of a new genus and subgenus. Bulletin of the British Museum (Natural History) Zoology Series **52**: 225–305.

Hoffmann M, Grubb P, Groves, CP, Hutterer R, van der Straeten E, Simmons N, Bergmans W. 2009. A synthesis of African and western Indian Ocean Island mammal taxa (Class: Mammalia) described between 1988 and 2008: an update to Allen (1939) and Ansell (1989). *Zootaxa* **2205:** 1–36.

I**rwin DM, Kocher TD, Wilson AC. 1991.** Evolution of the cytochrome-B gene of mammals. *Journal of Molecular Evolution* **32**: 128–144.

Jacobs DS, Babiker H, Bastian A, Kearney T, van Eeden R, Bishop JM. 2013. Phenotypic convergence in genetically distinct lineages of a *Rhinolophus* species complex (Mammalia, Chiroptera). *PLoS ONE* **8:** e82614.

Kaiser HF, 1974. Analysis of factorial simplicity. *Psychometrika* **39:** 31–36.

Kearney T, Volleth M, Contrafatto G, Taylor PJ. 2002. Systematic implications of chromosome GTG-band and bacula morphology for southern African *Eptesicus* and *Pipistrellus* and several other species of Vespertilionidae (Chiroptera: Vespertilionidae). *Acta Chiropterologica* **4**: 55–76.

Kerbis Peterhans JC, Fahr J, Huhndorf MH, Kaleme P, Plumtre AJ, Marks BD, Kizungu R. 2013. Bats (Chiroptera) from the Albertine Rift, eastern Democratic Republic of Congo, with the description of two new species of the *Rhinolophus maclaudi* group. *Bonn zoological Bulletin* **62:** 186–202.

Khan FAA, Phillips CD, Baker RJ. 2014. Timeframes of speciation, reticulation, and hybridization in the bulldog bat explained through phylogenetic analyses of all genetic transmission elements. *Systematic Biology* **63:** 96–110. doi:10.1093/sysbio/syt062

Kock D, Csorba G, Howell KM. 2000. *Rhinolophus maendeleo* n. sp. from Tanzania, a horseshoe bat noteworthy for its systematics and biogeography. *Senckenbergiana biologica* **80:** 233–239.

Kumar S, Stecher G, Tamura K. 2016. MEGA7: Molecular Evolutionary Genetics Analysis Version 7.0 for Bigger Datasets. *Molecular Biology and Evolution* **33:** 1870–1874.

Larkin MA, Blackshields G, Brown NP, Chenna R, McGettigan PA, McWilliam H, Valentin F, Wallace IM, Wilm A, Lopez R, Thompson JD, Gibson TJ and Higgins DG. 2007. ClustalW and ClustalX version 2. *Bioinformatics* **23:** 2947–2948.

Monadjem A, Richards L, Taylor PJ, Denys C, Dower A, Stoffberg S. 2013a. Diversity of Hipposideridae in the Mount Nimba massif, West Africa, and the taxonomic status of *Hipposideros lamottei*. *Acta Chiropterologica* **15:** 341–352.

Monadjem A, Richards L, Taylor PJ, Stoffberg S. 2013b. High diversity of pipistrelloid bats (Vespertilionidae: *Hypsugo, Neoromicia*, and *Pipistrellus*) in a West African rainforest with the description of a new species. *Zoological journal of the Linnean Society* **167:** 191–207.

Monadjem A, Taylor PJ, Cotterill FPD, Schoeman MC. 2010. *Bats of Southern and South-central Africa: A Biogeographic and Taxonomic Synthesis.* Johannesburg: Wits University Press.

Moore AE.Cotterill FPD, Key RM. 2017. A geomorphic and geological framework for the interpretation of species diversity and endemism in the Manica Highlands. *Kirkia* **19:** 54-69.

Moore AE, Cotterill FPD, Broderick T, Plowes D. 2009. Landscape evolution in Zimbabwe from the Permian to present: with implications for kimberlite prospecting. *South African Journal of Geology* **112:** 65-88.

Mutumi GL, Jacobs DS, Winker H. 2016. Sensory drive mediated by climatic gradients partially explains divergence in acoustic signals in two horseshoe bat species, *Rhinolophus swinnyi* and *Rhinolophus simulator*. *PLoS ONE* **11:** e0148053.

Nesi N, Nakouné E, Cruaud C, Hassanin A. 2011. DNA barcoding of African fruit bats (Mammalia, Pteropodidae). The mitochondrial genome does not provide a reliable discrimination between *Epomophorus gambianus* and *Micropteropus pusillus*. *Comptes Rendus Biologies* **334:** 544–554.

Nesi N, Kadjo B, Pourrut X, Leroy E, Pongombo Shongo C, Cruaud C, Hassanin A. 2013. Molecular systematics and phylogeography of the tribe Myonycterini (Mammalia, Pteropodidae) inferred from mitochondrial and nuclear markers. *Molecular Phylogenetics and Evolution* **66:** 126–137.

Odendaal LJ, Jacobs DS. 2011. Morphological correlates of echolocation frequency in the endemic Cape horseshoe bat, *Rhinolophus capensis* (Chiroptera: Rhinolophidae). *Journal of Comparative Physiology A.* **197:** 435-446.

Partridge TC. 1998. Of diamonds, dinosaurs and diastrophism: 150 million years of landscape evolution in southern Africa. *South African Journal of Geology* **101**: 3 167–184.

Partridge TC, Maud RR. 2000. The Cenozoic of Southern Africa. New York, Oxford Monographs on Geology and Geophysics. 406 pp.

Ralph TM, Richards LR, Taylor PJ, Napier MC, Lamb JM. 2015. Revision of Afro-Malagasy *Otomops* (Chiroptera: Molossidae) with the description of a new Afro-Arabian species. *Zootaxa* **4057:** 1–49.

Rohlf FJ. 2011. tpsRegr version 1.38. Ecology and Evolution, SUNY, Stony Brook.

Rolf FJ. 2013. tpsDig version 2.17. Ecology and Evolution, SUNY, Stony Brook.

Ronquist, F, Huelsenbeck JP. 2003. MRBAYES 3: Bayesian phylogenetic inference under mixed models. Bioinformatics **19**:1572–1574.

Schlick-Steiner BC, Steiner FM, Seifert B, Stauffer C, Christian E, Crozier RH. 2010. Integrative taxonomy: a multisource approach to exploring biodiversity. *Annual Review of Entomology* **55:**421–38.

Stoffberg S, Jacobs DS, Matthee CA. 2011. The Divergence of Echolocation Frequency in Horseshoe Bats: Moth Hearing, Body Size or Habitat? *Journal of Mammalian Evolution* **18:** 117–129.

Stoffberg S, Schoeman MC, Matthee CA. 2012. Correlated genetic and ecological diversification in a widespread southern African horseshoe bat. *PLoS ONE* **7:** e31946.

Tavare S. 1986. Some probabilistic and statistical problems on the analysis of DNA sequences. *Lecture Notes on Mathematical Modelling in the Life Sciences* **17**: 57–86.

Taylor PJ, Stoffberg S, Monadjem A, Schoeman MC, Bayliss J, Cotterill FPD. 2012. Four New Bat Species (*Rhinolophus hildebrandtii* Complex) Reflect Plio-Pleistocene Divergence of Dwarfs and Giants across an Afromontane Archipelago. *PLoS ONE* **7**.

Vallo P, Benda P, ČervenÝ J, Koubek P. 2013. Conflicting mitochondrial and nuclear paraphyly in small-sized West African house bats (Vespertilionidae). *Zoologica Scripta* **42**: 1–12.